

DATE ISSUED JUN 5 1970

ORNL/CSD/TM-87

790-30

Production Control in HTGR Fuel Rod Fabrication

D. J. Downing
Milton Bailey

OAK RIDGE NATIONAL LABORATORY
OPERATED BY UNION CARBIDE CORPORATION · FOR THE DEPARTMENT OF ENERGY

Printed in the United States of America. Available from
National Technical Information Service
U.S. Department of Commerce
5285 Port Royal Road, Springfield, Virginia 22161
Price: Printed Copy \$6.50; Microfiche \$3.00

This report was prepared as an account of work sponsored by an agency of the United States Government. Neither the United States Government nor any agency thereof, nor any of their employees, contractors, subcontractors, or their employees, makes any warranty, express or implied, nor assumes any legal liability or responsibility for any third party's use or the results of such use of any information, apparatus, product or process disclosed in this report, nor represents that its use by such third party would not infringe privately owned rights.

ORNL/CSD/TM-87
Dist. Category UC-77

Contract No. W-7405-eng-26

COMPUTER SCIENCES DIVISION

10

PRODUCTION CONTROL IN HTGR FUEL ROD FABRICATION

D. J. Downing and Milton Bailey*

(Sponsor: G. W. Westley; Originator: D. J. Downing)

*Consultant, University of Tennessee, Knoxville, Tennessee

NOTICE

This document contains information of a preliminary nature.
It is subject to revision or correction and therefore does
not represent a final report.

Date Published - June, 1979

UNION CARBIDE CORPORATION, NUCLEAR DIVISION
operating the

Oak Ridge Gaseous Diffusion Plant . Oak Ridge National Laboratory
Oak Ridge Y-12 Plant . Paducah Gaseous Diffusion Plant

for the
DEPARTMENT OF ENERGY

ACKNOWLEDGMENTS

We would like to thank David Needham and Betsy Horwedel for their programming assistance, E. J. Allen, P. Angelini, S. R. McNeany of the Metals and Ceramics Division for their programmatic assistance necessary for this work, and Collene Trammell and Carol Bullard for typing the report.

CONTENTS

LIST OF FIGURES	vii
LIST OF TABLES.	viii
ABSTRACT.	1
I. INTRODUCTION	3
II. METHODS FOR DETECTING CHANGES IN PROCESS OPERATING LEVEL . .	7
III. A FEEDBACK CONTROL EXAMPLE	16
IV. DATA ANALYSIS.	22
Campaign Two	24
Campaign Three	25
Campaign Four.	25
V. CLASSICAL DESIGN	41
VI. OTHER QUALITY CONTROL METHODS.	56
SUMMARY	68
REFERENCES.	71
APPENDIX A	73
APPENDIX B.	87



LIST OF FIGURES

<u>Figure</u>	<u>Page</u>
1. Schematic Diagram of Control Scheme for Fuel Rod Fabrication	5
2. Example of Process Drift in Production of Fuel Rods.	9
3. Schematic of the Fourdrinier Papermaking Process	16
4. Block Diagram of the Control Scheme.	21
5. Plot of the Campaign Two and One-Step-Ahead Forecasts Using the ARIMA(4,0,18) Model.	26
6. Plot of Campaign Three and One-Step-Ahead Forecasts Using the ARIMA(17,0,0) Model.	27
7. Plot of Campaign Four and One-Step-Ahead Forecasts Using the ARIMA(2,0,0) Model	29
8. Simulation of Campaign Two With Delay Value $B=1$	32
9. Simulation of Campaign Two With Delay Value $B=20$	33
10. Simulation of Campaign Three With Delay Value $B=1$	34
11. Simulation of Campaign Three With Delay Value $B=20$	35
12. Simulation of Campaign Four With Delay Value $B=1$	36
13. Simulation of Campaign Four With Delay Value $B=20$	37
14. Simulation of Unstable Process With Delay Value $B=1$	39
15. Simulation of Unstable Process With Delay Value $B=20$	40
16. Deterministic Block Diagram of the System.	42
17. Open Loop Transfer Function of the System.	47
18. The Bode Plot.	49
19. Step Function Response For Proportional Control.	50
20. The Simulations Diagram (Classical Design)	51
21. Step Function Response For the Classical Design.	53
22. Simulation Diagram (Box-Jenkins Design).	54
23. Step Function Response For the Box-Jenkins Design.	55
24. Distribution of Chance Variations (x) in a Sample Measure of Quality	58
25. Control Chart for x	58
26. Cumulative Sum of $(x_i - k)$ Plotted Against Number of Samples Using a V-mask	62

LIST OF TABLES

<u>Table</u>	<u>Page</u>
1. Simulation Case Studies.	8
2. Average Number of Rods Before Slope/Step Was Statistically Significant.	11
3. Total Number of Rods Produced Before Change Was Detected.	13
4. Descriptive Statistics for Campaigns Two, Three, and Four	24
5. Comparison of Mean Square Errors for Controlled and Uncontrolled Processes	38
6. Comparison of Control Chart Methods.	67

PRODUCTION CONTROL IN HTGR FUEL ROD FABRICATION

D. J. Downing and Milton Bailey*

ABSTRACT

The purpose of this report is twofold: (1) To determine which techniques are capable of detecting drift or step changes earliest in a manufacturing process. The techniques of interest are the Kalman Filter, weighted least squares, and Shewhart control chart. (2) What method, or methods, would work well in maintaining the manufacturing process at an acceptable level of quality?

To solve part (1) above, simulation studies were performed for various test cases of interest. These test cases varied the degree of shift as well as the process and measurement variation. Step changes were also included in the simulations. No single technique was superior in all of these cases, but the Kalman Filter appeared to be more robust to various process changes. The weighted least squares did a good job when the weight was near unity (0.9977) and failed when the weight was small (0.63). The Shewhart control chart is better for detecting step changes than for trends. Thus, depending on the type of change one would expect in the process, he might choose any one of the above methods.

Several methods were compared to try to answer part (2). Given the target value that one wishes his product to attain and accurate measuring devices, the deviation from target can be computed. The object of control theory is to force the deviation from target as near to zero as possible. The criterion by which this is done is to minimize the mean square error of forecasted future values. If we can forecast what the process will do, then we can take compensatory action to correct it. Obviously, the better the forecasting, the better the control will be. Thus, the first problem is to build a model that will accurately forecast the deviation from target. In this report the model building and forecasting was done using the methods of Box and Jenkins [1]. To illustrate the process employed by Box and Jenkins, an example of optimal control theory applied to a papermaking process is given. Following this is the analysis of fuel rod length data from three fuel rod production campaigns. These campaigns are indicative of the data that will be produced when fuel rod production begins. Thus, it was of interest to see if the data lent itself to time series analysis and, in particular, to the method of Box and Jenkins. It was found that all three campaigns could be adequately modeled by difference equation models which were fit to the data. To show how control theory would decrease the deviation from target

*Consultant, University of Tennessee, Knoxville, Tennessee

of these campaigns, simulations were run using the models derived from the real data. (The program for generating the simulations is given in Appendix A.) The control in the rod length problem is the height of the carbon shim pinch valve setting. Lowering or raising the pinch valve will decrease or increase the rod length. The response to this control is immediate; but since measurement may not be done until later, two delay values were employed. The values were one time-unit and 20 time-units. In essence, one has to forecast ahead the length of the delay value. Thus, in one control problem, a one-step-ahead forecast was made, while in another, a twenty-step-ahead forecast was made. It is clearly shown that little control is affected when the delay value is 20. In fact, this is the most important result of this part of the study. The control will tend to decrease as the time increases. For stable process (i.e., ones which vary about some target value and do not drift away), the control is almost nonexistent when the delay time is as large as 20 periods. Thus, decreasing the time to measuring the rod lengths would enhance the control capabilities considerably. To show more dramatically the effect a control can have, a non-stationary process was simulated. This process drifted considerably away from target, but the controlled process stayed very close to the target. This was especially true when the delay time was one.

A drawback to the Box-Jenkins procedure is that the process must be modeled before control can be affected. In the three campaigns analyzed, the models were distinct—implying that the control algorithm is distinct for each campaign. The campaigns were acceptable in that they produced rods of acceptable length—thus, the Box-Jenkins approach may be too sensitive for control in fuel rod production. A method that does not have this problem is the classical control theory approach. Both approaches are similar in their effect on the process. The results using the classical approach are exemplified by simulations obtained using CSMP (Continuous System Modeling Program). The programs used in the simulations are contained in Appendix A.

Alternative control methods to the Box-Jenkins and classical control schemes were presented since the processes studied are stable over time. These control methods are not dynamic in that they do not change the input to bring the output back to target. Rather, they are primarily visual and present a chart that shows the process over time. These charts have control limits that indicate when the process is in control or out-of-control. These methods may be adequate for many processes, especially if the process is stable over time and changes gradually. The methods (Shewhart control charts and Cumulative sum chart) are compared under various conditions to ascertain which type of control chart is best (best in terms of early warning of the process going out of control). In general, it is found that cumulative sum charts (CUSUM) are superior to Shewhart charts except when large changes in the process occur.

I. INTRODUCTION

Quality control of a process is a necessary and vital part of good manufacturing. The quality of a product can be monitored by measuring various characteristics which directly affect its usefulness. These measurements can be compared to control limits. If the measurements fall within the control limits, the process is said to be "in control" and manufacturing continues. Once observations fall outside the control limits, the process is declared "out of control" and manufacturing ceases until the problem is rectified and the process is back in control.

Good measurement systems and sophisticated estimation techniques (e.g., least squares, Kalman Filtering) can be used in predicting the true level of the process. These estimation techniques can be used to indicate process changes like step changes or drift. Both estimates of the change (say drift) and tests of hypothesis concerning its true value can be performed. If a change is observed and detected by the measurement system, then appropriate modifications can be made to the process. Thus, good measurement systems serve three purposes: (1) accurate measure of process level (for example, fuel rod length and fuel rod fissile assay), (2) early warning of process change, and (3) indicate process modifications (i.e., control).

Several techniques exist that can be used in estimating process change. Two well-known techniques are least squares and Kalman Filtering. It should be pointed out that for a stationary system, a Kalman Filter model can be constructed to yield the same results as those given by least squares. The difference is in the algorithm that generates the solution. Thus, any least squares model can be modeled by Kalman Filtering. In

certain cases where the type of process change is known, a model that describes that type of change can be estimated using least squares or Kalman Filtering, and the parameters tested to see if they are significant. For example, one can hypothesize a linear drift model:

$$y_t = a + bt + \epsilon_t$$

where

y_t = measured value at time t

ϵ_t = random error associated with the t^{th} measurement

a = intercept (process mean if $b=0$)

b = slope (or drift parameter).

At each time, t , a test of the hypothesis that the drift is zero ($H_0: b=0$) can be made. If we do not reject the hypothesis, we conclude that there is no drift and the process has not changed.

Some questions of interest concerning these techniques are: (1) How soon will the Kalman Filter or least squares detect a drift of given size? (2) How soon will they detect a step change? (3) Under what circumstances would one technique be preferred over the other? These questions are the focus of the next section.

Given that one has a technique to estimate the true level of the process, how can this estimate be used to control the process? Quality control charts have been used since the early 1960s. These charts plot the data and give visual cues as to the quality of the product. Trends, jumps, or drift away from the target value are easily seen and appropriate remedies to bring the process back into "control" can be made. In many cases, key variables can be identified which directly affect the quality

of the product. For example, the amount of carbon shim particles directly affects the length of fuel rods. If the length of the fuel rod is a characteristic of interest, it can be controlled by adjusting the amount of shim particles used, or if fuel rod fissile control is of interest, it can be controlled by adjustment of the fissile particle volumetric dispenser. If the transfer function relating the input variable to the output variable is known, then a feedback control scheme can be implemented which uses this information to keep the process in control. Figure 1 is a schematic diagram of a control scheme for fuel rod fabrication.

ORNL-DWG 79-7679

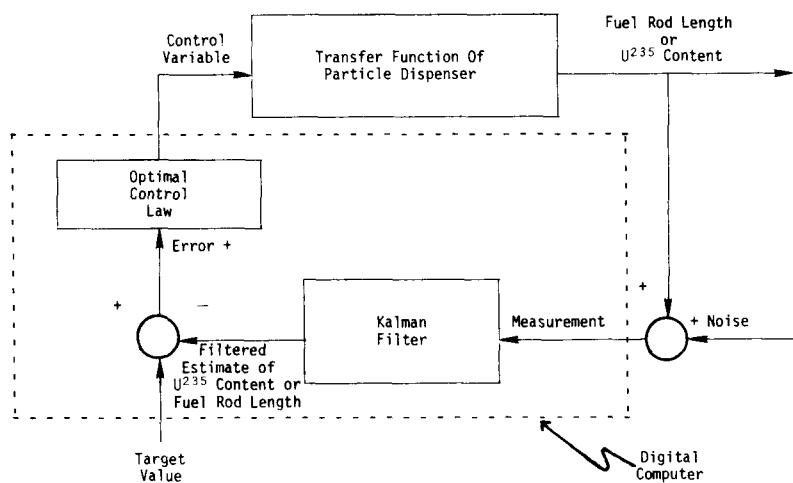


Fig. 1. Schematic Diagram of Control Scheme for Fuel Rod Fabrication.

Starting at the lower right corner of the diagram, one observes a measurement (in this case, a measurement of the U^{235} content) that includes a noise contribution. The noisy measurement is then filtered to yield an unbiased estimate of the true U^{235} content. This estimated value is subtracted from the target value to obtain an estimate of deviation from target. This deviation is used together with the control variable, transfer function, and optimal control law to produce an adjustment to the control variable that will either increase or decrease the U^{235} content and attempt to maintain the deviation from target as close to zero as possible. In this report we shall investigate feedback control schemes. One scheme is that presented by Box and Jenkins [1] which uses models that describe the process and indicate how control is to be exerted. Another approach is given by the "classical" system design in which the control algorithm is to be designed by modeling the system as a first-order linear system and minimizing the system error consistent with system stability. These techniques exert control after each sample point. In this sense they may be called continuous control schemes. If the process is stable and varies little over time, continuous control may not be necessary. Other quality control schemes such as Shewhart control charts or cumulative sum charts (CUSUM) can be used under these conditions. These control charts serve as early warning systems and indicate when control may be necessary. Another feature of control charts is their relative simplicity in comparison to the Box-Jenkins or classical design approaches.

II. METHODS FOR DETECTING CHANGES IN PROCESS OPERATING LEVEL

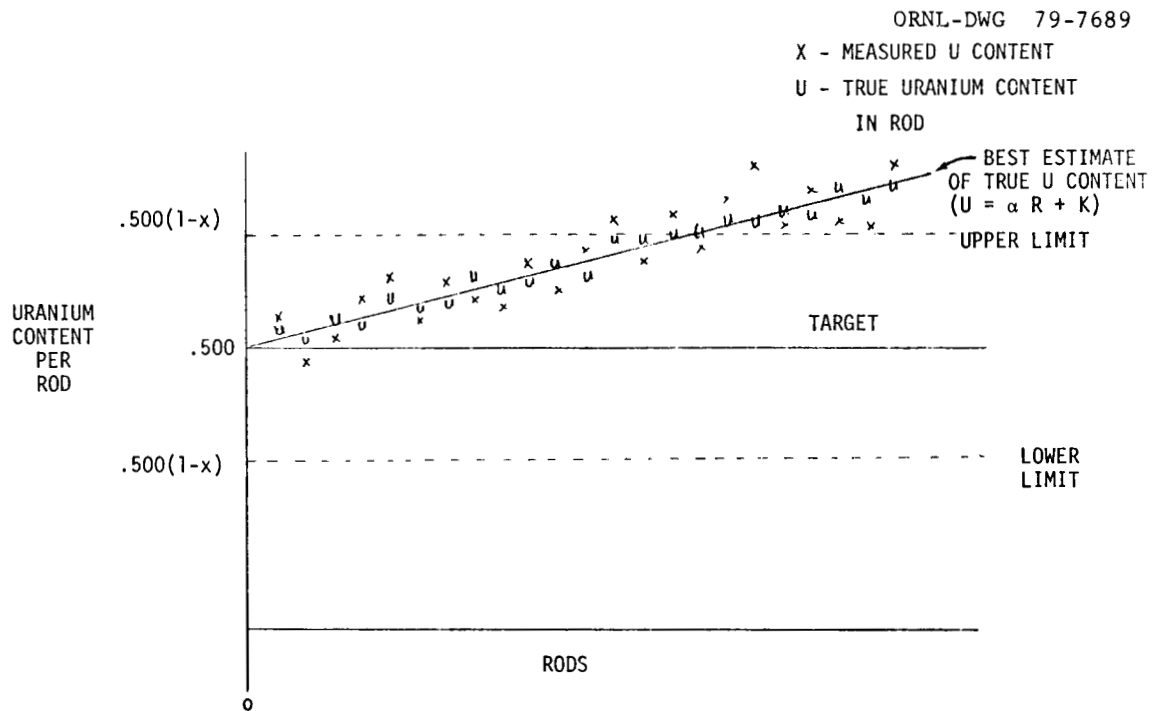
Early detection of changes in the process operating level afford one the time to make appropriate compensating changes to control variables and, thus, bring the operating level back to normal. Several techniques are available that yield estimates of the true operating level. The usefulness of a technique depends on the type of change one expects the process to make. For example, the Kalman Filter is designed to detect small constant changes in the process level; the weighted least squares is appropriate to detect trends in the level of a process; and the Shewhart control chart will detect large changes best. No one scheme is best in all cases. Knowing how the process operates and the types of changes most likely to occur will generally guide one to a wise choice.

Simulations were performed using Kalman Filter, weighted linear least squares, and the Shewhart control chart in order to compare the methods and in order to then utilize the equations such that operating parameters such as speed of fissile assay, source size, and number of rods assayed could be better estimated for equipment in a refabrication facility. The simulation cases studied are given below in Table 1. The simulated general problem of concern is shown in Fig. 2. The picture represents the fissile content of fuel rods on the vertical axis and rod number along the horizontal axis. As we go from left to right, it is assumed that the fissile content is increasing linearly with time. The solid horizontal line extending from the 0.5 gm. mark on the vertical axis is the "target" value, that is, the fissile content we are trying to produce. The dashed lines extending from $0.5(1-x)$ gms. and $0.5(1+x)$ gms. are lower and upper control limits, respectively. They are the values

such that, if the process level goes below or above them, rods of inferior quality are being produced. The x's indicate a measured fissile content and the u's indicate the true fissile content. The straight line drawn through the points is the least squares line which gives the best estimate of the true fissile content if the process has a linear drift. One question of interest is which of the methods of estimation will detect this trend earliest? The answer to this question is affected by three factors. The first is the magnitude of the trend. Does one method perform better if the slope is small compared to another, or is one method uniformly better regardless of the magnitude of the slope? The other factors deal with the variability of the process and the measuring equipment. Process error is that associated with the true rod length. In Fig. 2 it is the process error that causes the u's to vary about the mean drift line. Compounding the problem is the measurement noise caused by the inaccuracy of the measuring device.

Table 1. Simulation Case Studies.

Simulation	Process Parameters			
	Slope/Step	Value	Process Error(%)	Measurement Error(%)
1	Slope	2.5E-05	0.5	2.0
2	Slope	5.0E-06	0.5	2.0
3	Slope	1.0E-06	0.5	2.0
4	Slope	2.5E-05	0.5	5.0
5	Slope	5.0E-06	0.5	5.0
6	Slope	1.0E-06	0.5	5.0
7	Slope	2.5E-05	1.0	0.1
8	Slope	5.0E-06	1.0	0.1
9	Slope	1.0E-06	1.0	0.1
10	Step	0.01	0.5	2.0
11	Step	0.01	0.5	5.0
12	Step	0.01	1.0	0.1



MEASURED URANIUM CONTENT NORMALLY DISTRIBUTED ABOUT TRUE
URANIUM CONTENT WITH A STANDARD DEVIATION OF $\pm A \%$

TRUE URANIUM CONTENT NORMALLY DISTRIBUTED ABOUT MEAN
DRIFT LINE WITH A STANDARD DEVIATION OF $\pm B \%$

Fig. 2. Example of Process Drift in Production of Fuel Rods.

Process and measurement error combine to make detection of a change in process level slower, especially if the change is small in comparison to the variability. The situation in Table 1 that is not reflected in Fig. 2 is the step change. A step change occurs when the process jumps from one level to another instantaneously. This type of change may not be picked up well by weighted linear least squares if the weight is near one since this tends to estimate the trend as an average of several past

observations. A smaller weight would discard past observations and emphasize the most current ones. Thus, the jump would affect the estimate more in this case and detection would be sooner.

Answers to the question of which method to choose is further complicated by our lack of knowledge of what the process will do. Are we sure that we will see a linear trend, or might the level changes come from a series of random jumps? This concern caused us to use the Kalman Filter to estimate the true level of the process and not specifically estimate a trend parameter. The Kalman Filter is a state estimation technique whose power lies in its ability to model systems easily and is computationally efficient. Thus, it can be used to calculate estimates of the trend exactly the same as those given by weighted least squares. The only difference between the two is in the algorithm used to obtain the answer. Thus, although we used linear least squares as a method of detection, we could have replaced it by the Kalman Filter specifically modeled to detect linear drift. The equations describing the Kalman Filter algorithm is given in Appendix B.

The answers to the above questions are contained in Table 2 which contains the results of the simulations. The three columns on the left of Table 2 describe the simulation study parameters (i.e., measurement error, process error, and slope/step value).

Listed under each of the methods of detection is the average number of rods plus or minus its standard deviation before the slope/step was determined to be significant.. Entries not listing a standard deviation are the results of a single simulation; thus, no estimate could be calculated. Only one simulation was performed in those cases where the method

Table 2. Average Number of Rods Before Slope/Step Was Statistically Significant.

Measurement Error	Process Error	Slope/Step	Value	Method of Detection			
				Least Squares		Kalman Filter	Control Chart
				$\alpha = 0.63$	$\alpha = 0.9977$		
2.0	0.5	Slope	2.5 E-05	28972	157 ± 84	133 ± 64	136 ± 97 (N=5/10)
2.0	0.5	Slope	5.0 E-06	16172	396 ± 284	294 ± 195	167 ± 141 (N=31/50)
2.0	0.5	Slope	1.0 E-06	5029	2872 ± 2014	827 ± 668	619 ± 421 (N=10/10)
5.0	0.5	Slope	2.5 E-05	>30,000	230 ± 195	203 ± 134	273 ± 198 (N=5/10)
5.0	0.5	Slope	5.0 E-06	14881	391 ± 687	442 ± 359	352 ± 323 (N=8/10)
5.0	0.5	Slope	1.0 E-06	3622	13032	1406	1212
0.1	1.0	Slope	2.5 E-06	8498	85 ± 46	80 ± 34	69 ± 40 (N=4/10)
0.1	1.0	Slope	5.0 E-06	6763	309 ± 129	233 ± 147	132 ± 71 (N=5/10)
0.1	1.0	Slope	1.0 E-06	14461	825 ± 622	549 ± 290	326 ± 237 (N=8/10)
2.0	0.5	Step	0.01	27 ± 2 (N=3/6) ^a	36 ± 19	34 ± 9	35 ± 20 (N=11/11)
5.0	0.5	Step	0.01	2038 (N=1/3) ^a	71 ± 47	74 ± 40	207 ± 66 (N=2/10)
0.1	1.0	Step	0.01	>10,000 (N=0/3)	28 ± 2	27 ± 9	—

^aExceeded 10,000 runs without detecting change

appeared unable to detect the process change rapidly. In other cases the number of times a simulation was repeated was 10 unless denoted otherwise. The expression (N=8/10) represents that 10 simulations were performed, but only 8 yielded results. The reason for this is that if detection was not obtained within 30,000 observations, the simulation was stopped. Thus, in some cases the slope/step change was not detected within this limit, indicating that the method either catches the shift early or not at all. The mean and standard deviation are based on those simulations that stopped before the 30,000 observation limit.

Conclusions that can be reached from the simulations are:

- 1) The Kalman Filter detects drift in the process better than weighted least squares or the Shewhart control chart when measurement error dominates.

- 2) The Shewhart control chart is best for detecting drift when measurement error is less than process error.
- 3) The Kalman Filter and weighted least squares (with weight $\alpha = 0.9977$) detect step changes equally well.
- 4) The Shewhart control chart is better for detecting step changes than for trends.
- 5) The ability of weighted least squares to detect a trend in the process decreases drastically as the weight decreases (and, hence, incorporates fewer past observations).

The above conclusions imply that the Kalman Filter may be the best detector for most cases. Two additional reasons to suggest its use are: (1) its modeling capability is superior to the weighted least squares, and (2) it is computationally efficient. As can be seen by the above conclusions, no one method is best for all cases. Thus, it may be necessary to employ more than one technique.

In addition to the above results, the question of how well the detection techniques work after the process has been running for a considerable time must be investigated. A partial answer to the question is given in Table 3, which describes the times to detection after the process has been running for various lengths of time. Besides the time to detection, given various startup times, it was of interest to see what effect various weights would have on the detection capabilities of weighted least squares using a linear model. It was conjectured that, if the process ran for a long time, then a small weight might be best for detecting step changes due to the "lack of memory" induced by the small weight, i.e., the most present observations would have the largest effect.

Table 3. Total Number of Rods Produced Before Change Was Detected*

Simulation #	DELAY PERIODS											
	10 Rods		500 Rods		1000 Rods		10,000 Rods					
	KF	WLS ([†] 0.9999)	KF	WLS (0.9999)	KF	WLS(0.9999)	KF	WLS (0.9999)	WLS (0.95)	WLS (0.90)	WLS (0.85)	Shewhart CC
1	12	11	580	534	1088	1024	10045	10049	14215	14599	>15000	10014
2	12	12	552	511	1062	1050	10001	10062	>15000	>15000	>15000	10003
3	12	51	540	521	1040	1038	10207	10091	10014	10006	11529	10018
4	11	85	555	528	1092	1017	10227	10151	>15000	>15000	10006	10021
5	18	26	597	539	1058	1010	10001	10127	10019	10006	>15000	10003
6	24	24	554	521	1075	1028	10168	10109	10013	11007	10005	10085
7	20	11	513	502	1033	1025	10124	10083	10009	10899	>15000	10028
8	21	20	535	536	1069	1026	10116	10097	10014	>15000	13386	10050
9	19	25	536	546	1016	1054	10056	10112	10006	>15000	>15000	10003
10	27	11	549	550	1001	1019	10003	10165	10015	>15000	>15000	10073
Average	17.6	27.6	551.1	528.8	1053.4	1029.1	10094.8	10104.6	10538.1**	11303.4**	11231.5**	10029.8

* Simulation of a process with mean 10.0, standard deviation of 1.0, and a step decrease of 1 unit at the specified delay period.

† Value inside the parenthesis is the weight used in the weighted least squares.

** Average is based upon the values that were observed; thus, they are biased downwards and should not be used for comparison.

Thus, a rapidly occurring change like a step change would be detected faster since the previous observations would be ignored. Table 3 is split into two parts; the left section comparing the detection capabilities given various run times (or delay periods) before the jump occurs, and the right section comparing the effect of varying the weight given that the process has produced 10,000 rods.

Investigating the left section of Table 3, if the number of rods before the jump occurs is important, then we might expect to find either an increase or decrease in the number of rods to detection. Subtracting off the delay period gives the number of rods before detection. Thus, for the Kalman Filter we observe, on the average, 7.6, 51.1, 53.4, and 94.8 rods before we detect the change when the corresponding delay periods are 10, 500, 1000, and 10,000. Similarly, using weighted least squares to estimate the linear model (with weight 0.9999), the average number of rods until detection was 17.6, 28.8, 29.1, and 104.6 corresponding to delay periods 10, 500, 1000, and 10,000. This indicates that the detection time increases as the delay period increases for either method. Intuitively, this might be expected since past experience indicates no change — the longer this period lasts, the more reluctant we are to expect or detect a change. It is consoling to note that the number of rods to detection is not directly proportional to the delay time; rather, it appears to be proportional to the logarithm of the delay time.

The right half of Table 3, under the delay period of 10,000 rods, indicates the effect of decreasing the weight used in the weighted least squares analysis. The significance of the slope parameter of the linear model, estimated using weighted least squares, was tested for each new

rod after the delay period. The average number of rods until detection for the weights 0.95, 0.90, and 0.85 are not comparable since the step change was not detected for these weights in one or more of the simulation runs. The number of simulations in which detection did not occur (within 5,000 rods) increases as the weight decreases. This indicates that the "lack of memory" induced by the weights either works well or not at all in detecting a step change. This can be seen most dramatically for the weight of 0.95. In one simulation, the shift was detected at rod 14,215; in two simulations, the shift was never detected, but in the other simulations, the detection was much faster than most of the other schemes. This indicates that there may exist some optimal weight which will detect a shift in the process faster than, say, the Kalman Filter.

In addition to the weighted least squares and Kalman Filter detection schemes, the simple Shewhart control chart was employed. The process was said to be out of control if two consecutive observations exceeded the two-sigma warning lines. Table 3 shows that this method is clearly superior to the others, detecting the shift an average of 29.8 rods later. This suggests that more than one detection technique should be employed in detecting a shift in the process. As pointed out earlier, the Shewhart control chart is best for detecting step changes, and these simulations clearly back up that statement. Since we have no *a priori* knowledge of what type of shift (if any) will occur in the manufacturing process, it would be wise to use two of the detection schemes — one which is best for detecting drift and one which is best for detecting step changes.

These methods for detection indicate how the process is running. They can be joined with control algorithms that will enable one to keep

the process on target. The next section deals with an example that shows how control of a process can be obtained and maintained.

III. A FEEDBACK CONTROL EXAMPLE

An enlightening example is given in a paper by Tee and Wu [2] concerning the control of a papermaking process. Their goal is to control the paper basis weight. Figure 3 presents a schematic of the Fourdrinier papermaking process.

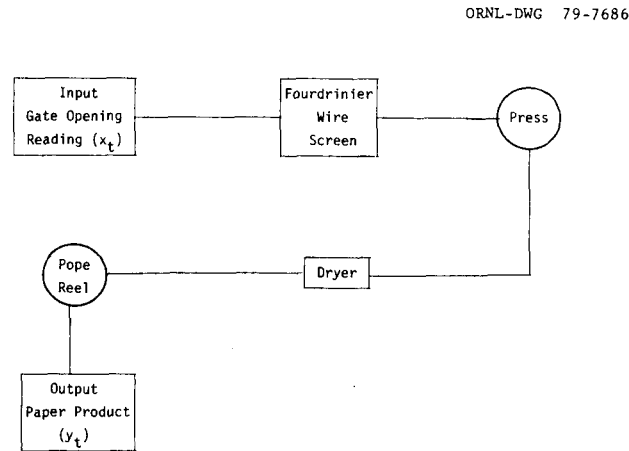


Fig. 3. Schematic of the Fourdrinier Papermaking Process.

The input into the system is controlled by opening or closing the stock gate located in the mixing box. By increasing the stock gate opening, the paper basis weight is increased. They assumed that the system could be described by:

$$\begin{bmatrix} \text{deviation} \\ \text{from} \\ \text{target} \end{bmatrix} = \begin{bmatrix} \text{impulse} \\ \text{response} \\ \text{function} \end{bmatrix} \times \begin{bmatrix} \text{referenced} \\ \text{regulated} \\ \text{value} \end{bmatrix} + \begin{bmatrix} \text{disturbance} \\ \text{effect} \end{bmatrix}$$

or mathematically,

$$Y_t = (V_0 + V_1B + V_2B^2 + \dots)(X_{t-1} - \bar{X}) + N_t, \quad (1)$$

where,

Y_t = deviation from target at time t ,

X_t = referenced stock gate value at time t ,

\bar{X} = mean stock gate value,

B = backward shift operator, e.g., $BY_t = Y_{t-1}$, and

V_j = j^{th} impulse response weight.

N_t is the process noise at time t which makes perfect control impossible. By holding the control variable, X_t , constant at its steady state value (the value at which the output should be on target), a realization of the process noise, N_t , is obtainable. This noise may be modeled by the techniques outlined by Box and Jenkins [1]. Tee and Wu found that N_t satisfied the following model:

$$N_t = \phi N_{t-1} + a_t, \quad (2)$$

where ϕ is an unknown constant, and a_t is an unobservable random variable, generally taken to be white noise (i.e., normally distributed with mean zero and variance σ_a^2).

Having identified the form of the noise model, the next step was to identify the transfer function relating the input (stock gate value) to the output (paper basis weight). Their analysis revealed the following transfer function model:

$$Y_t = V_0(X_{t-1} - \bar{X}) + N_t. \quad (3)$$

The other weights, V_1, V_2, \dots , given in Equation (1) are zero, and we see that the deviation from target is directly related to the deviation of the regulated value from its mean. If the difference between X_{t-1} and \bar{X} were unity for all time, then V_0 may be interpreted as the gain of the system. Combining the noise model (Equation (2)) and the transfer function model (Equation (3)), one obtains the combined dynamic-disturbance model:

$$Y_t = V_0(X_{t-1} - \bar{X}) + \frac{1}{1 - \phi B} a_t . \quad (4)$$

Using 160 data points, they estimated the unknown parameters V_0 and ϕ to be $\hat{V}_0 = 1.0991$ and $\hat{\phi} = 0.8511$.

A control plan was set up which required that the output deviations be kept to a minimum. The theoretical objective is to keep the output deviations at zero, i.e., $Y_t = 0$ for all t . Since the model is

$$Y_t = V_0(X_{t-1} - \bar{X}) + N_t ,$$

when $Y_t = 0$, then

$$V_0(X_{t-1} - \bar{X}) = -N_t .$$

Shifting ahead one time period, we see that

$$X_t - \bar{X} = -\frac{1}{V_0} N_{t+1} . \quad (5)$$

Let ΔX_t represent the adjustment in the control variable at time t , i.e.,

$$\begin{aligned} \Delta X_t &= X_t - X_{t-1} \\ &= (X_t - \bar{X}) - (X_{t-1} - \bar{X}) = -\frac{1}{V_0} (N_{t+1} - N_t) . \end{aligned} \quad (6)$$

At time $(t-1)$ we need to estimate N_t , and at time t , we need to estimate N_{t+1} . Using these forecasts, we can estimate ΔX_t , our change in the control variable at time t . We choose the forecasts of N_t and N_{t+1} so as to minimize the mean square forecast error. Any linear combination of these optimal forecasts will also be optimal in the sense of mean square error. Thus, ΔX_t is an optimal control. It can be shown that the optimal one-step-ahead forecast of N_t is

$$\hat{N}_{t-1}(1) = \phi a_{t-1} + \phi^2 a_{t-2} + \phi^3 a_{t-3} + \dots = \frac{\phi}{(1-\phi B)} a_{t-1} . \quad (7)$$

Similarly, at time t , the optimal one-step-ahead forecast of N_{t+1} is

$$\hat{N}_t(1) = \frac{\phi}{(1-\phi B)} a_t . \quad (8)$$

Thus, the change in the control variable at time t is

$$\Delta X_t = -\frac{1}{V_0} \left(\hat{N}_t(1) - \hat{N}_{t-1}(1) \right) . \quad (9)$$

If one substitutes the optimal one-step-ahead forecast $\hat{N}_{t-1}(1)$ into Equation (5) and then uses this to estimate the error in the output, we find

$$Y_t = V_0 \left(-\frac{1}{V_0} \hat{N}_{t-1}(1) \right) + N_t = N_t - \hat{N}_{t-1}(1) . \quad (10)$$

Thus, the error in the output at time t is simply the forecast error at lead time 1 for the N_t process. That is,

$$N_t - \hat{N}_{t-1}(1) = a_t ,$$

and, hence,

$$Y_t = a_t . \quad (11)$$

Using Equations (7), (8), (9), and (11), we find that

$$\Delta X_t = -\frac{1}{V_0} \left(\frac{\phi}{1-\phi B} \right) (a_t - a_{t-1}) = -\frac{1}{V_0} \left(\frac{\phi}{1-\phi B} \right) (Y_t - Y_{t-1}) . \quad (12)$$

Substituting $\hat{\phi} = 0.8511$ and $\hat{V}_0 = 1.0991$, the control Equation (12) becomes

$$\Delta X_t \cong 0.85\Delta X_{t-1} - 0.77(Y_t - Y_{t-1}) . \quad (13)$$

To see how the control equation works, we proceed as follows. Assume ΔX_0 and $Y_0 = 0$, then the control action ΔX_t can be easily calculated whenever Y_t is observed. Following Tee and Wu [2], if we observe

$$Y_1 = -0.4 ,$$

then we adjust the stock gate opening upward by

$$\Delta X_1 = -0.77Y_1 = 0.308 .$$

Continuing, if we observe

$$Y_2 = -0.1 ,$$

then we again increase the opening by

$$\Delta X_2 = 0.85\Delta X_1 - 0.77(Y_2 - Y_1) = 0.0308 ,$$

and so on. This model building and feedback control scheme is summarized in Fig. 4. Studying Fig. 4 will be important for later discussion. The schematic clearly shows the different parts needed in designing a feedback control scheme.

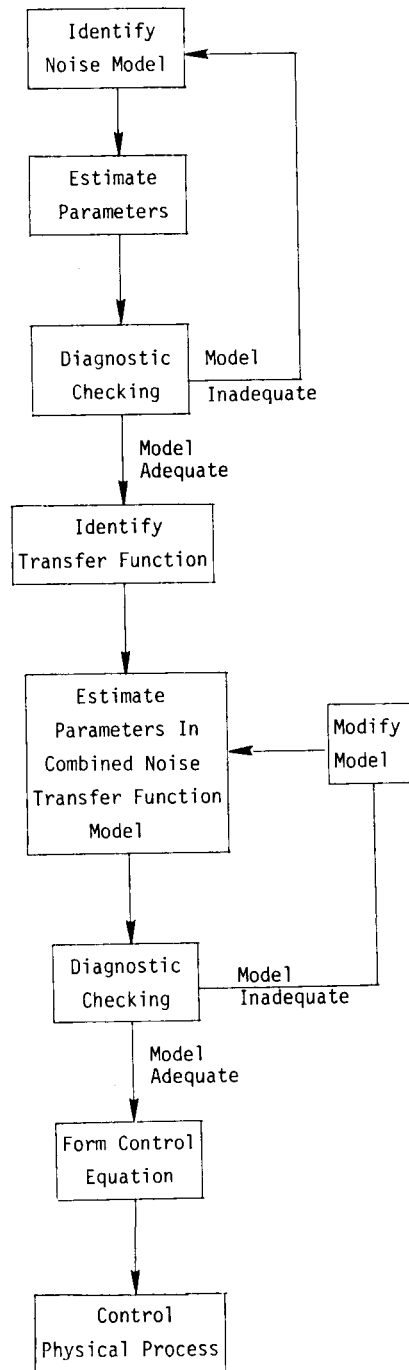


Fig. 4. Block Diagram of the Control Scheme.

IV. DATA ANALYSIS

In this section, we discuss the identification of the noise model for the fuel rod lengths. Data on three separate campaigns is analyzed, and an appropriate model that describes the stochastic process is chosen for each campaign. These models are used later in the simulation study. Since many changes in the fuel rod fabrication process were made between campaigns, the models representing these campaigns were expected to change, and no comparison is made between them.

In each of these campaigns, the pinch valve setting was kept at a constant level, thought to produce rods of length 1.94 inches. Keeping the pinch valve at a constant level allows one to investigate the noise process, N_t . We assume that the noise process N_t will follow an autoregressive-integrated-moving average (ARIMA) model. These models are amply described in [1]. The results of our analyses shall simply be reported for each campaign without rederiving the work of Box and Jenkins. In what follows, let N_t denote the t^{th} observed rod length minus the target value 1.94, a_t an unobservable white noise random variable, and B the backward shift operator (equivalent to Z^{-1} in sampled-data control theory). Then the ARIMA (p,d,q) model is written as:

$$(1 - \phi_1 B - \phi_2 B^2 - \dots - \phi_p B^p) \nabla^d N_t^* = (1 - \theta_1 B - \theta_2 B^2 - \dots - \theta_q B^q) a_t \quad (14)$$

where $\nabla = (1 - B)$ and $N_t^* = (N_t - \mu)$ if $d = 0$; otherwise $N_t^* = N_t$. For example, an ARIMA (1,1,1) model could be written as

$$(1 - \phi_1 B)(1 - B)N_t = (1 - \phi_1 B)a_t \quad (15)$$

Expanding the above, we have

$$[1 - (1 + \phi_1)B + \phi_1 B^2]N_t = (1 - \theta_1 B)a_t ,$$

or

$$N_t - (1 + \phi_1)N_{t-1} + \phi_1 N_{t-2} = a_t - \theta_1 a_{t-1} . \quad (16)$$

The methods of Box and Jenkins in analyzing time series follows three basic steps in an iterative fashion. Step 1 identifies what ARIMA model (or models) best describes the data. There may be more than one tentative model. The second step is to estimate the parameters of the tentative model(s). The third step is to test the adequacy of the model. If the model is adequate, the analysis may stop, but if the model is inadequate, we go back to Step 1 and reiterate the process.

A fourth step could be the use of the ARIMA model to forecast and/or control the process. Table 4 gives the simple descriptive statistics for each campaign. The mean rod lengths are very close to the target value (1.94) for all three campaigns. The standard deviations are comparable for all campaigns, and their magnitude indicates the precision of the process. The coefficients of variation indicate that the campaigns are nearly identical in their precision. The autocorrelations indicate the degree of internal association as well as a means to identifying the appropriate ARIMA model.

Several tentative models were explored. In this report, we shall simply list the ARIMA models that best fit the data. The models below are the best in the sense of minimum mean square error. Additionally, the assumption that the errors $\{a_t\}$ are independent was tested and found to be satisfied in each case.

Table 4. Descriptive Statistics for Campaigns Two, Three, and Four.

ORNL-DWG 79-7688

Table 3. Descriptive Statistics for Campaigns Two, Three, and Four.

	Campaign Two	Campaign Three	Campaign Four
Sample Size	176	300	187
Mean	1.958	1.950	1.968
Standard Deviation	0.00774	0.01023	0.01015
Coefficient of Variation	0.40%	0.52%	0.52%
Autocorrelations			
lag 1	0.16	0.38	0.31
lag 2	0.21	0.30	0.29
lag 3	0.09	0.35	0.24
lag 4	0.23	0.34	0.20
lag 5	0.12	0.31	0.21
lag 6	0.18	0.30	0.18
lag 7	0.05	0.33	0.12
lag 8	0.19	0.34	0.17
lag 9	0.03	0.34	0.06
lag 10	0.20	0.34	0.13

Campaign Two

The model chosen for campaign two is ARIMA(4,0,18) with several of the parameters constrained to be zero. The model is:

$$(1 - \phi_2 B^2 - \phi_4 B^4)(N_t - \mu) = (1 - \theta_{17} B^{17} - \theta_{18} B^{18})a_t, \quad (17)$$

and the parameter estimates (with their standard errors beneath them in parenthesis) are:

$$(1 - 0.193B^2 - 0.206B^4)(N_t - 0.0177) = (1 - 0.142B^{17} + 0.212B^{18})a_t \quad (18)$$

$$(\underline{+0.076}) \quad (\underline{+0.076}) \quad (\underline{+0.001}) \quad (\underline{+0.080}) \quad (\underline{+0.080}) .$$

Writing Equation (18) out explicitly, we have:

$$N_t = 0.011 + 0.193N_{t-2} + 0.206N_{t-4} + a_t - 0.142a_{t-17} + 0.212a_{t-18} . \quad (19)$$

The standard deviation associated with the residuals $\{a_t\}$ is $\hat{\sigma}_a = 0.0072$. A plot of the campaign two series and the one-step-ahead predicted values using Equation (19) is given in Fig. 5.

Campaign Three

The model chosen for campaign three is ARIMA(17,0,0) with several of the parameters constrained to be zero. The model is:

$$(1 - \phi_1 B - \phi_3 B^3 - \phi_4 B^4 - \theta_{11} B^{11} - \phi_{17} B^{17})(N_t - \mu) = a_t \quad (20)$$

with parameter estimates,

$$(1 - 0.201B - 0.145B^3 - 0.1115B^4 - 0.137B^{11} - 0.123B^{17})(N_t - 0.0117) = a_t$$

$$\begin{array}{cccccc} (+0.059) & (+0.059) & (+0.061) & (+0.059) & (+0.056) & (+0.002) \end{array} \quad (21)$$

Rewriting the above, we have:

$$N_t = 0.003 + 0.201N_{t-1} + 0.145N_{t-3} + 0.115N_{t-4}$$

$$+ 0.137N_{t-11} + 0.123N_{t-17} + a_t \quad (22)$$

The estimated standard deviation of the residuals $\{a_t\}$ is $\hat{\sigma}_a = 0.0088$. A plot of this series and those predicted by the model given by Equation (22) is given in Fig. 6.

Campaign Four

The model that best fits the campaign four series is the ARIMA(2,0,0) model given by:

$$(1 - \phi_1 B - \phi_2 B^2)(N_t - \mu) = a_t \quad (23)$$

PLOT OF CAMPAIGN TWO AND ONE-STEP-AHEAD FORECASTS
 USING THE ARMA(4,18) MODEL

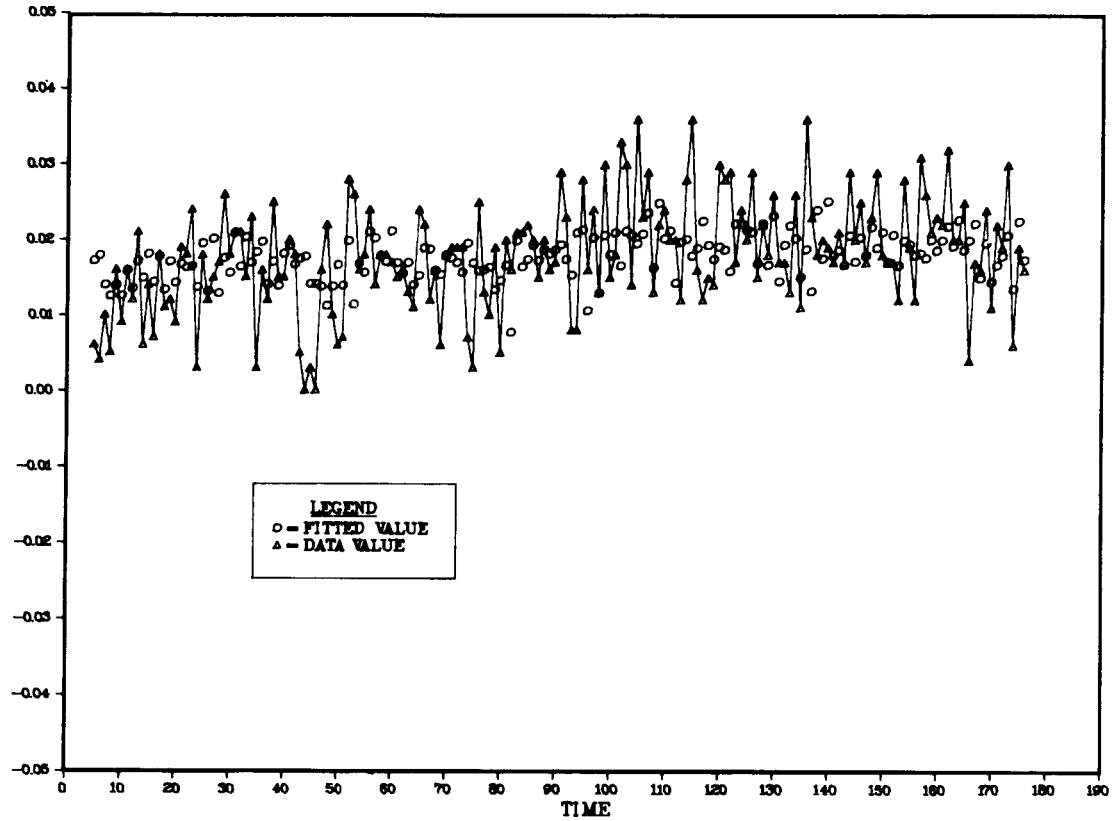


Fig. 5. Plot of Campaign Two and One-Step-Ahead Forecasts Using the ARIMA(4,0,18) Model.

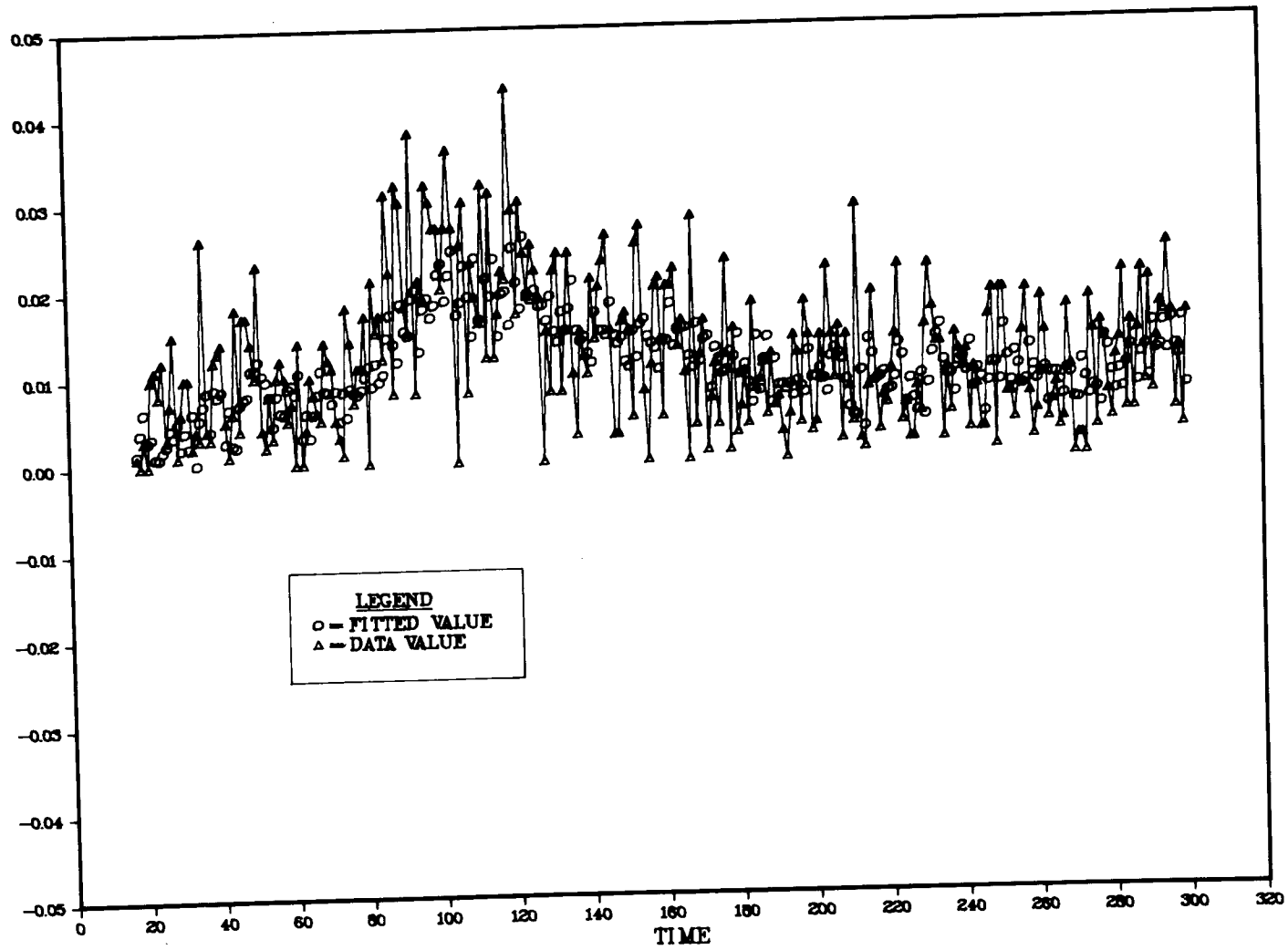


Fig. 6. Plot of Campaign Three and One-Step-Ahead Forecasts Using the ARIMA(17,0,0) Model.

The parameter estimates and their standard errors are:

$$(1 - 0.252B - 0.227B^2)(N_t - 0.028) = a_t \quad , \quad (24)$$

$$(\pm 0.073) \quad (\pm 0.074) \quad (\pm 0.001)$$

or equivalently,

$$N_t = 0.015 + 0.252N_{t-1} + 0.227N_{t-2} + a_t \quad . \quad (25)$$

The estimated standard error of the residual series is $\hat{\sigma}_a = 0.0094$. A plot of the campaign four series and the one-step-ahead predictions obtained by Equation (25) are given in Fig. 7.

The three models chosen for the three campaigns differ significantly in their form. This is probably due to changes in the process instituted between campaigns. In order to have an effective control system using the techniques presented by Box and Jenkins [1], the process cannot change over time as much as we have witnessed in these campaigns. These three campaigns allow us to model realistic simulations and show how feedback control can aid in keeping the process "in control".

In order to complete the control algorithm, we need to know the transfer function relating the pinch valve setting and the rod length. This data is not available in the campaigns discussed above. Additional experiments need to be performed in which the control variable is changed frequently so that its effect on the output can be determined. We will assume the simple transfer function identical to Tee and Wu's

$$Y_t = V_0(X_{t-b} \bar{X}) \quad (26)$$

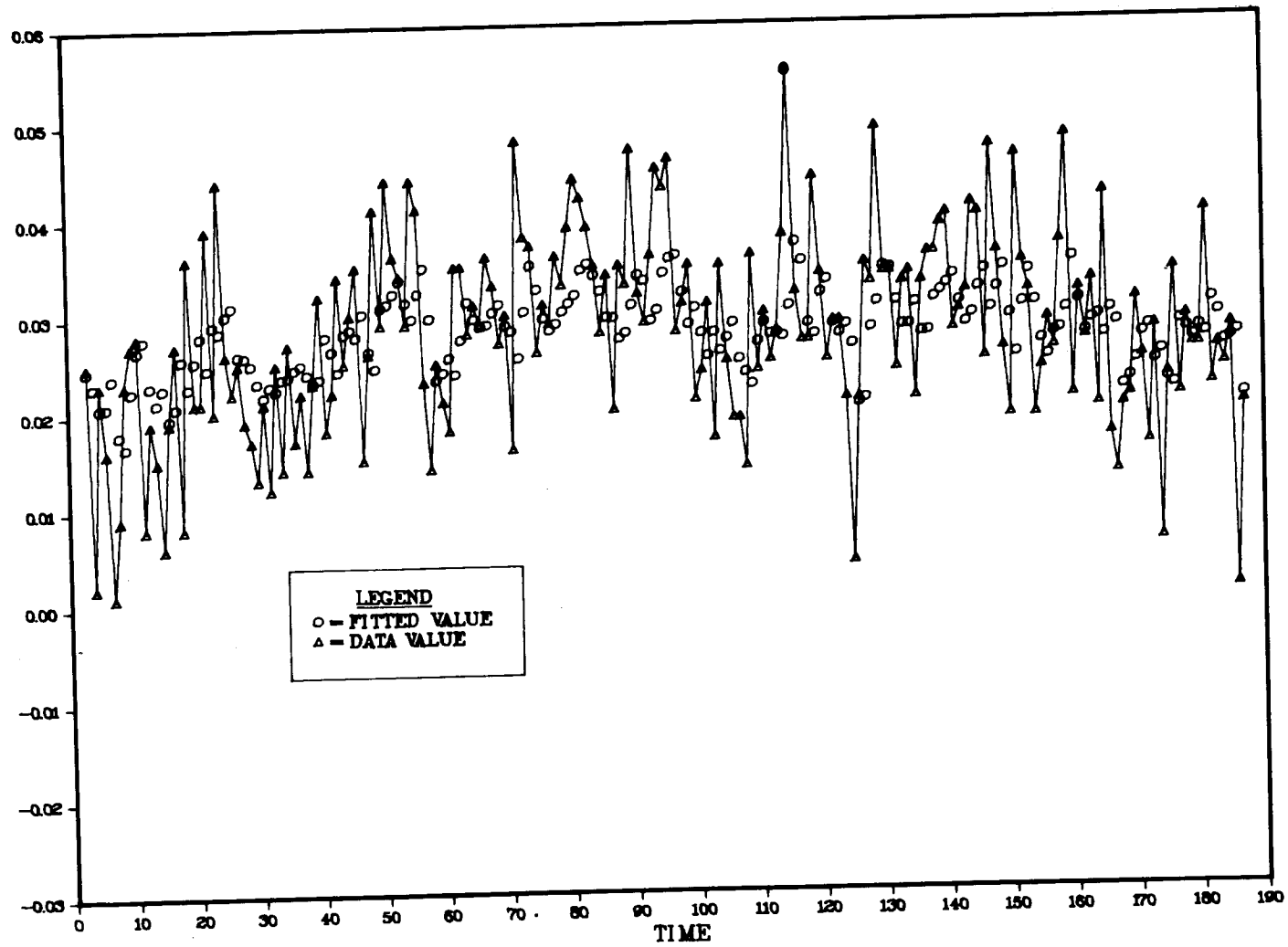


Fig. 7. Plot of Campaign Four and One-Step-Ahead Forecasts Using the ARIMA(2,0,0) Model.

where

Y_t = deviation of rod length from target at time t ,

X_t = pinch valve setting at time t ,

\bar{X} = mean pinch valve setting,

b = delay time,

and

V_0 = the impulse response weight.

The value of b indicates the amount of time that is required before a change in the control causes a change in the output. In the simulations studied, b was given the values 1 and 20. Although the effect of changing the pinch valve setting is immediate, there is the possibility of a long delay in the measuring of the rod length, thus the delay value $b = 20$. The value of V_0 was taken to be unity for the simulations and \bar{X} was set at zero for simplicity. Thus we were simulating the following process:

$$Y_t = X_{t-b} + N_t$$

where N_t is described by one of the following equations (19, 22, or 25).

For example, using Equation (25) we have:

$$N_t = 0.015 + 0.252N_{t-1} + 0.227N_{t-2} + a_t .$$

In simulating this process we randomly selected the value of a_t from a normal population with mean zero and variance equal to unity. Further, the a_t 's were chosen independently of each other. To obtain a realization of the process, we had to give starting values to N_{t-1} and N_{t-2} . Setting $t=1$ to start the process, we gave N_0 and N_{-1} the value zero. The reason for this is that N_t has mean zero and this would be our best guess of the

values of N_0 and N_{-1} . These initial values only affect the process for the first few time points. One would not notice any difference between a process initialized with $N_0 = N_{-1} = 0$ or one initialized with $N_0 = N_{-1} = 10$ after the initial 20 or 30 observations. To be sure of no startup effect, we dropped the first 100 observations from each simulation. The simulation runs are given in Figs. 8–13. Since the processes are stable, the control is minimal and large differences between the controlled processes are not apparent. A measure of the effectiveness of the control is the mean square error. The smaller the mean square error, the better the process is running; that is, the smaller the deviation of the process from its target value. Table 5 below indicates the mean square error for the uncontrolled and controlled processes and the percent decrease in the error for the controlled process. As can be seen from Table 5, the reduction in MSE is always greatest when the delay value is 1. No reduction is seen for the controlled process when the delay is 20, but this is an artifact of a short stable series. The control is slight when a delay of 20 periods is used and, thus, the controlled and uncontrolled processes appear the same. This does not mean that the control is ineffective. If the process drifts from target, the control will bring it back. No drift was employed in simulating the campaigns. To simulate a process with drift, we employed a simple nonstationary process given by

$$(1-0.6B)(1-B)N_t = a_t, \quad (27)$$

where a_t is normally distributed with mean zero and variance 1, and a_t and a_k are independent for $t \neq k$. This process is one which has no mean value and may wander off indefinitely in either direction.

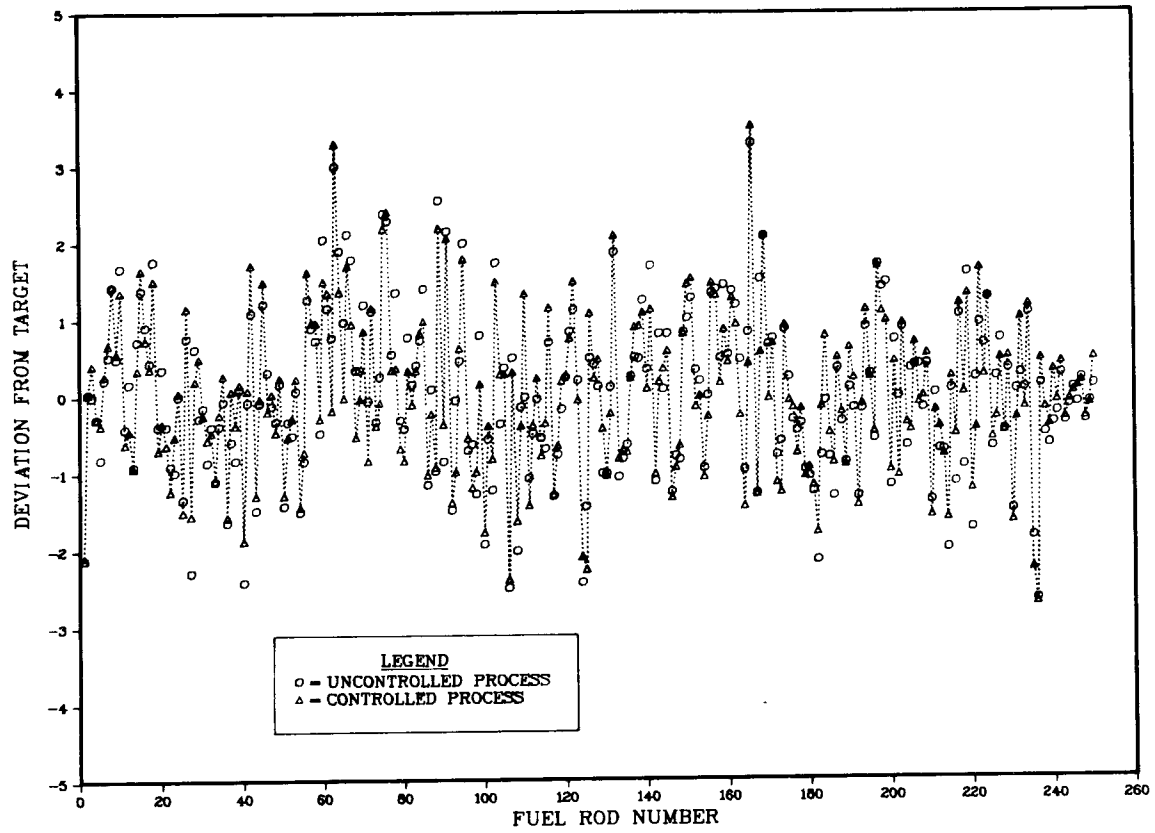


Fig. 8. Simulation of Campaign Two With Delay Value B=1.

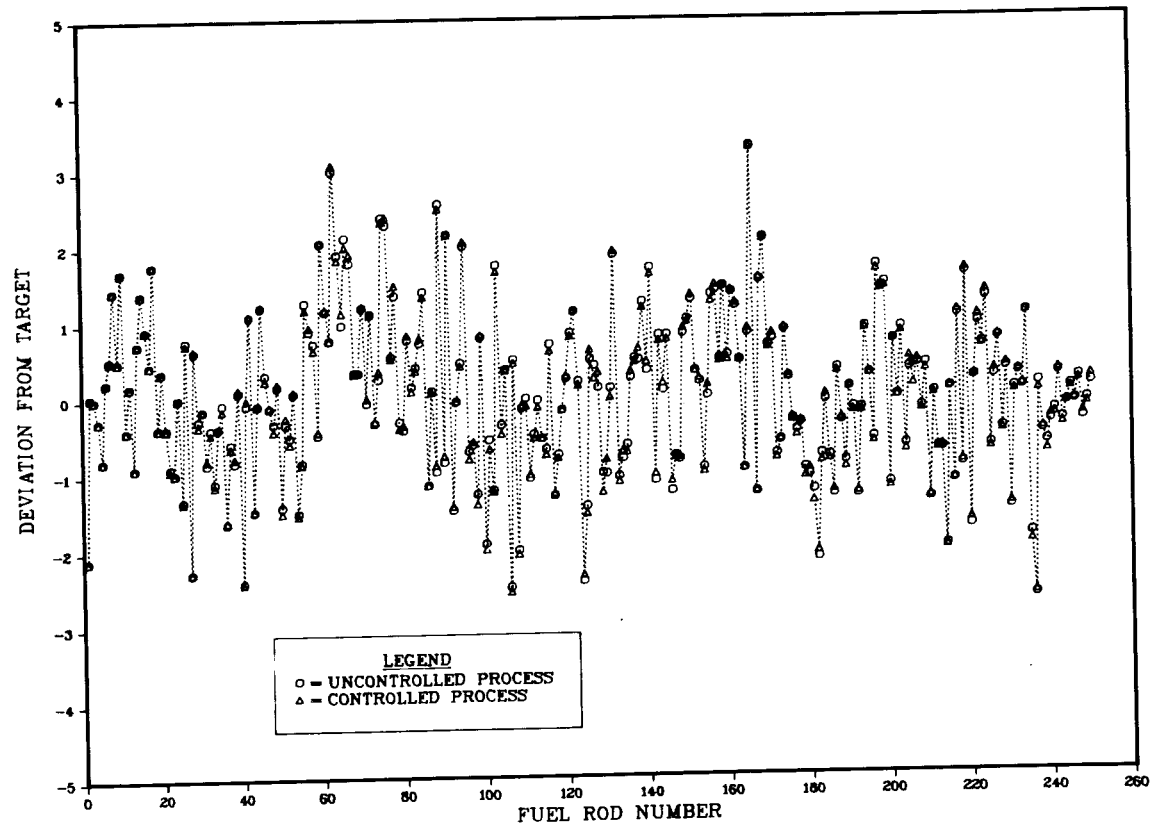


Fig. 9. Simulation of Campaign Two With Delay Value B=20.

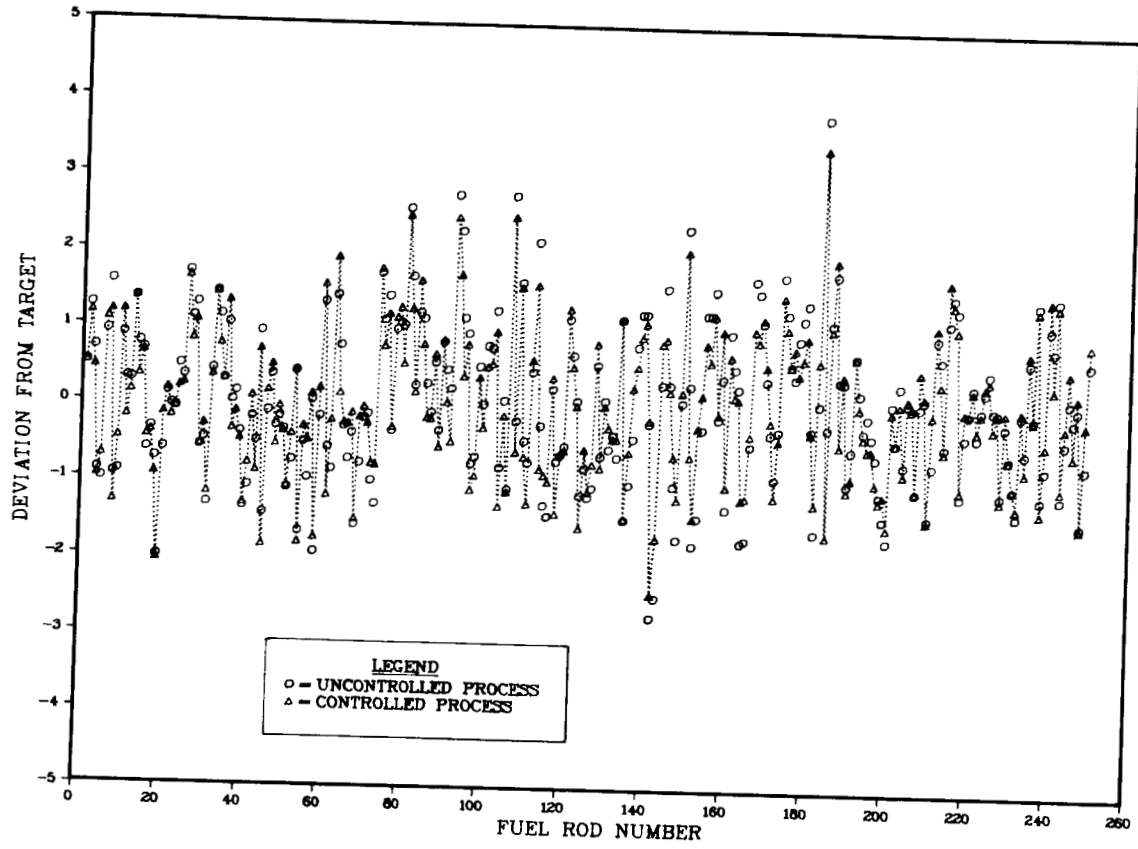


Fig. 10. Simulation of Campaign Three With Delay Value $B=1$.

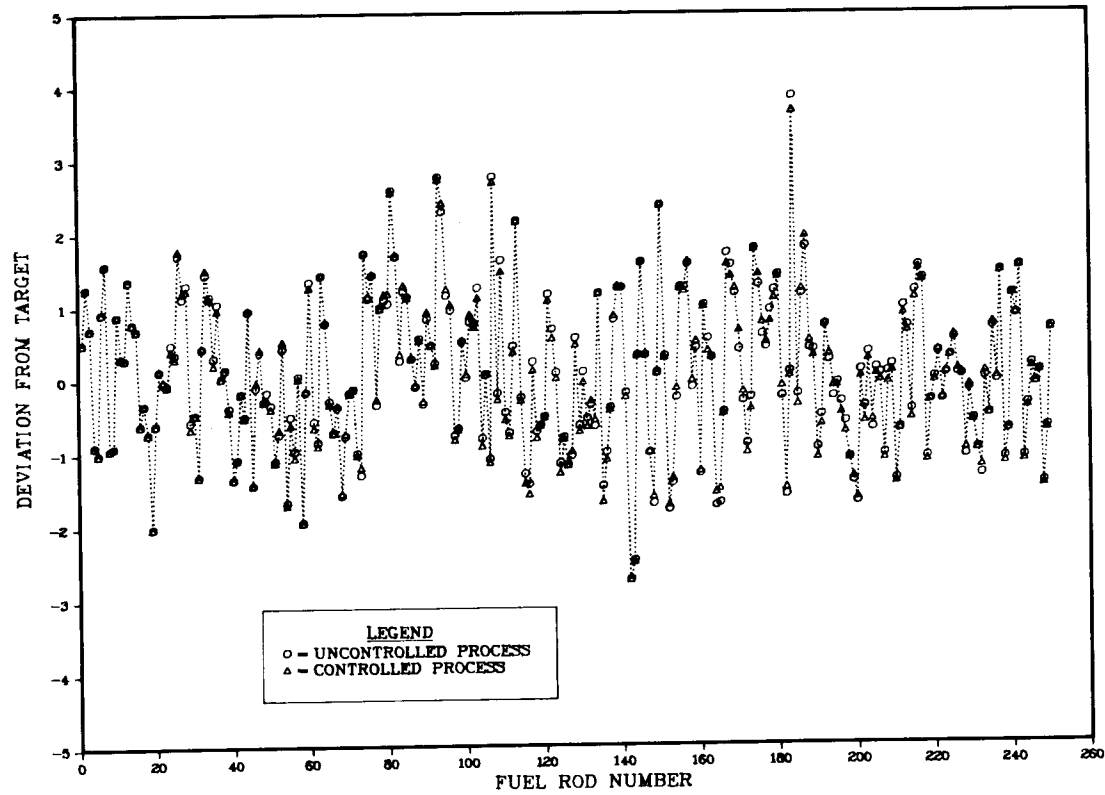


Fig. 11. Simulation of Campaign Three With Delay Value B=20.

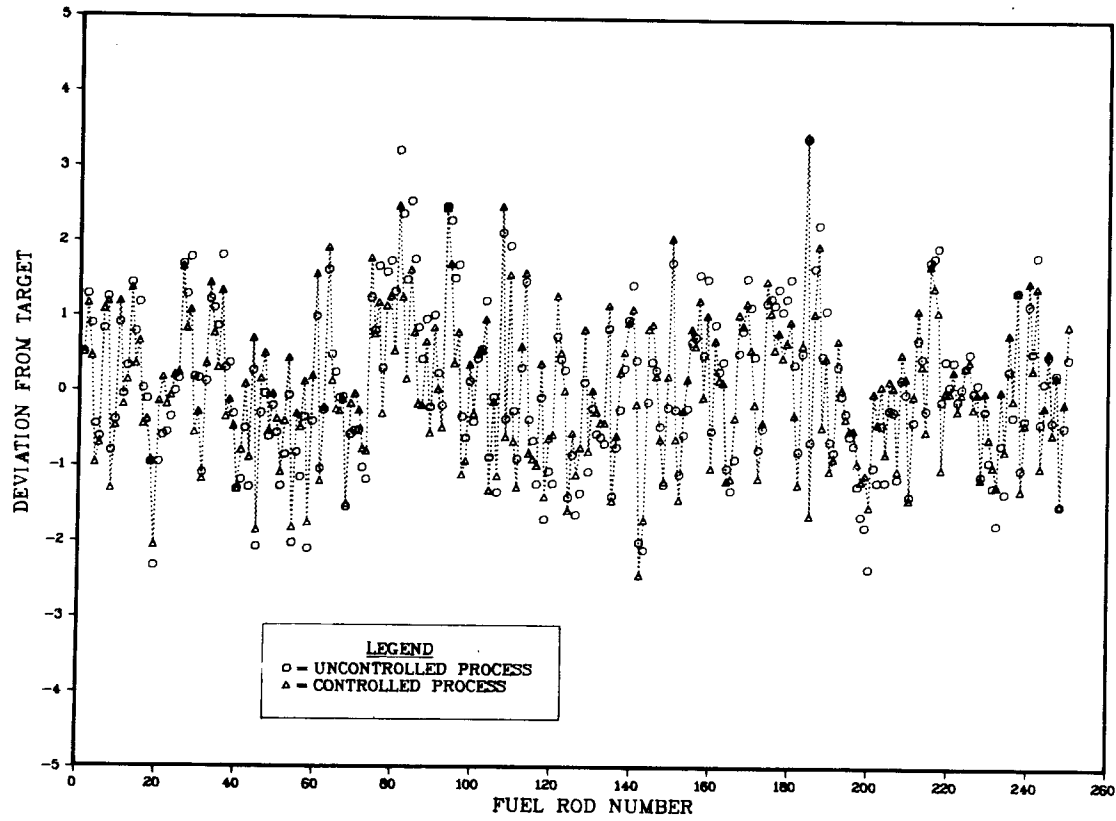


Fig. 12. Simulation of Campaign Four With Delay Value B=1.

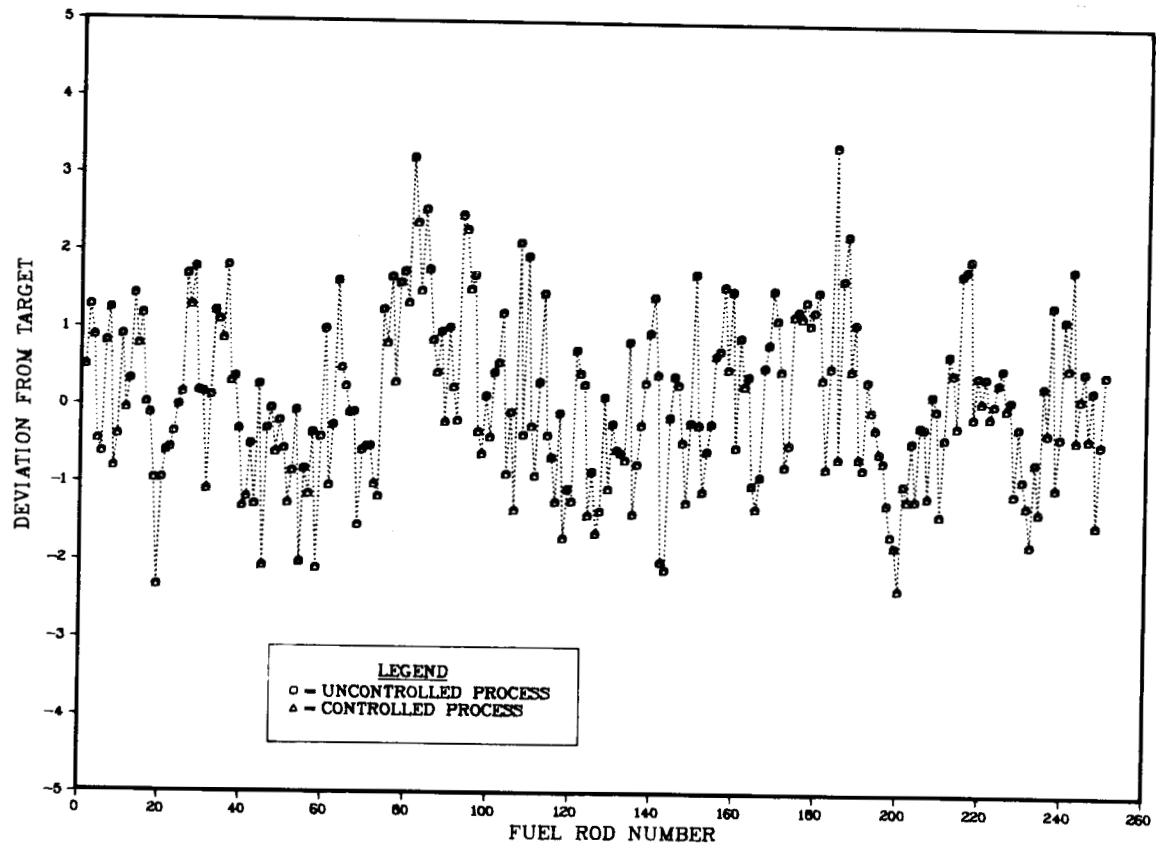


Fig. 13. Simulation of Campaign Four With Delay Value $B=20$.

Table 5. Comparison of Mean Square Errors for Controlled and Uncontrolled Processes.

Simulation	Delay Value	Uncontrolled Process MSE*	Controlled Process MSE	Percent** Reduction In MSE
Campaign 2	1	1.11	1.04	6.3
Campaign 2	20	1.11	1.13	-1.8
Campaign 3	1	1.07	0.92	14.0
Campaign 3	20	1.07	1.07	0.0
Campaign 4	1	1.17	0.92	21.4
Campaign 4	20	1.17	1.17	0.0
Nonstationary	1	437.93	0.92	99.8
Nonstationary	20	437.93	165.78	62.1

*MSE - Mean square error.

**Percent Reduction = (MSE Uncontrolled - MSE Controlled)/MSE Uncontrolled.

An indication of the effectiveness of the control algorithm in this unstable system is given in Figs. 14 and 15. The reduction in MSE is given at the bottom of Table 5. Note that, even with a delay of 20, the reduction in MSE is substantial. In Fig. 14 the delay time was $b = 1$, while in Fig. 15 the delay time was $b = 20$. The simulation with the long delay shows vividly that the control is sluggish while a short delay allows for rapid control of the process.

In summary, the following conclusions can be made:

- 1) The campaigns can be analyzed by the methods of Box and Jenkins.
- 2) To have an effective control system using the methods of Box and Jenkins, the models describing the process cannot change over time as much as we have witnessed in these campaigns.
- 3) The campaigns analyzed are stable and require very little control. This implies that not every item needs to be measured to insure

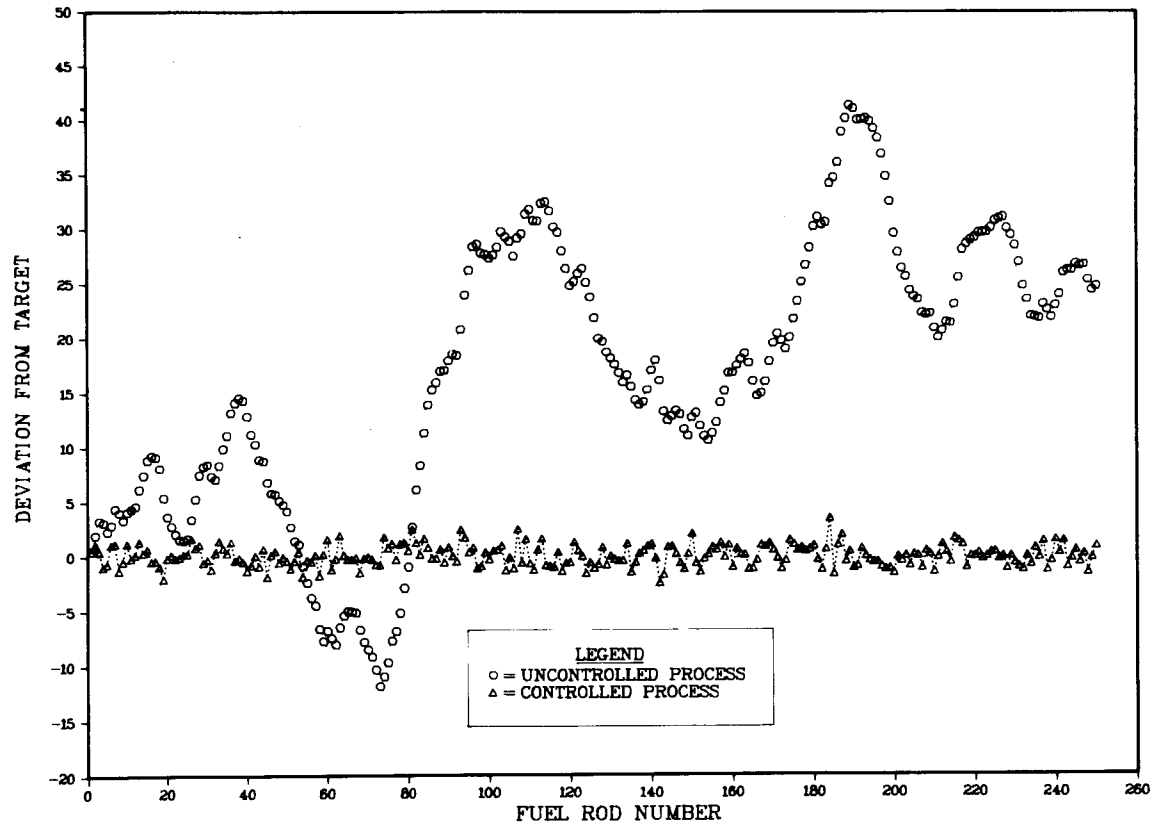


Fig. 14. Simulation of Unstable Process With Delay Value B=1.

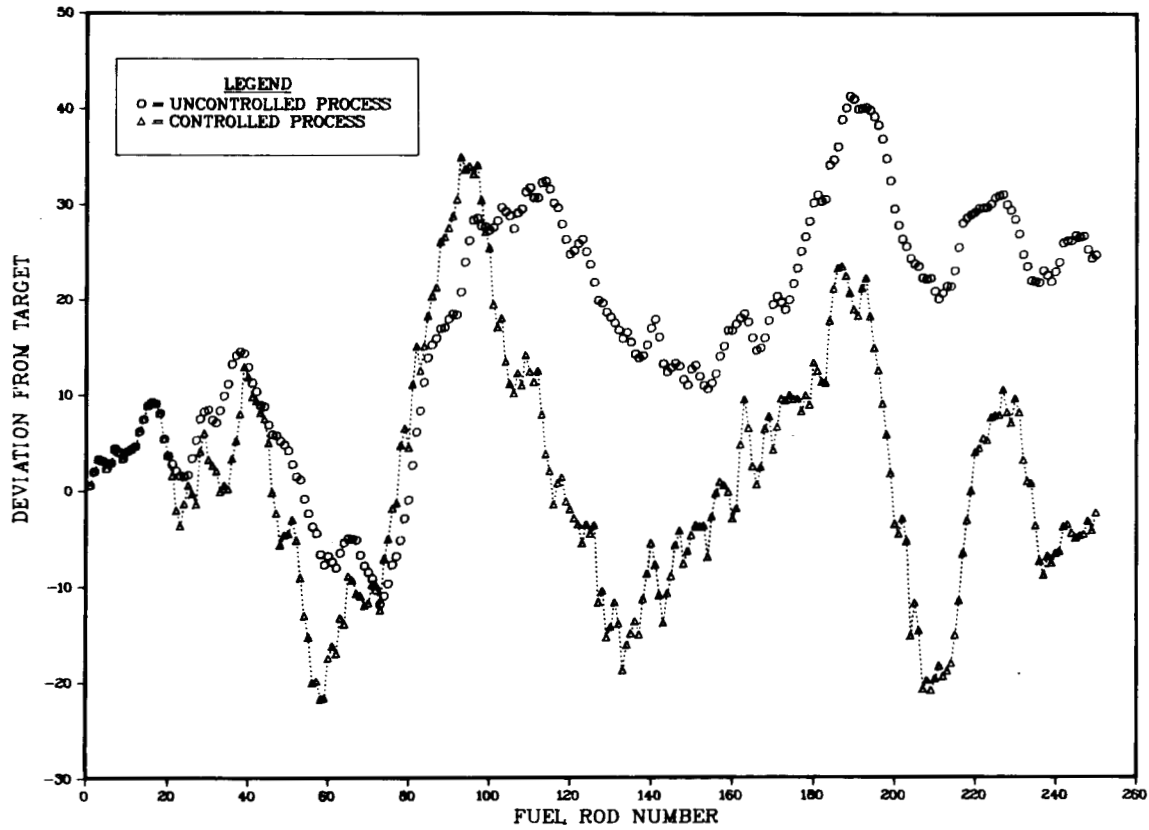


Fig. 15. Simulation of Unstable Process With Delay Value $B=20$.

good quality since the process does not change radically in a short time span.

- 4) The amount of control decreases rapidly as the delay value (the amount of time between a change in the input is observed in the output) increases.

V. CLASSICAL DESIGN

Some control techniques have the disadvantage that the transfer function relating the input variable to the output variable must be known. Classical techniques are available, however, that allow the effects of disturbances and modeling errors to be minimized, and in this section such a design procedure is outlined.

In designing the control scheme for the Fuel Rod Fabrication systems, we will consider it is characterized by the block diagram shown in Fig. 16. The classical control algorithm is to be designed from the viewpoint of a first-order process whose function is to minimize the system error consistent with system stability. We first consider the system as being continuous, i.e., the output variable and input variable are related by an ordinary linear differential equation. Defining the variables

y = fuel rod length

x = process disturbance

d = desired fuel rod length

e = system error = $d - y$,

the differential equation characterizing a first-order system can be expressed as

$$\frac{dy(t)}{dt} + ay(t) = K_p x(t) \quad (28)$$

where

$a \triangleq$ process time constant

$K_p \triangleq$ process gain.

As the production process changes, both "a" and " K_p " change, and any practical feedback control scheme must be relatively insensitive to the values of these parameters.

To illustrate, consider now a proportional controller whose action is described by the equation

$$e_c(t) = K_c e(t) \quad (29)$$

where $e_c \triangleq$ output of the controller.

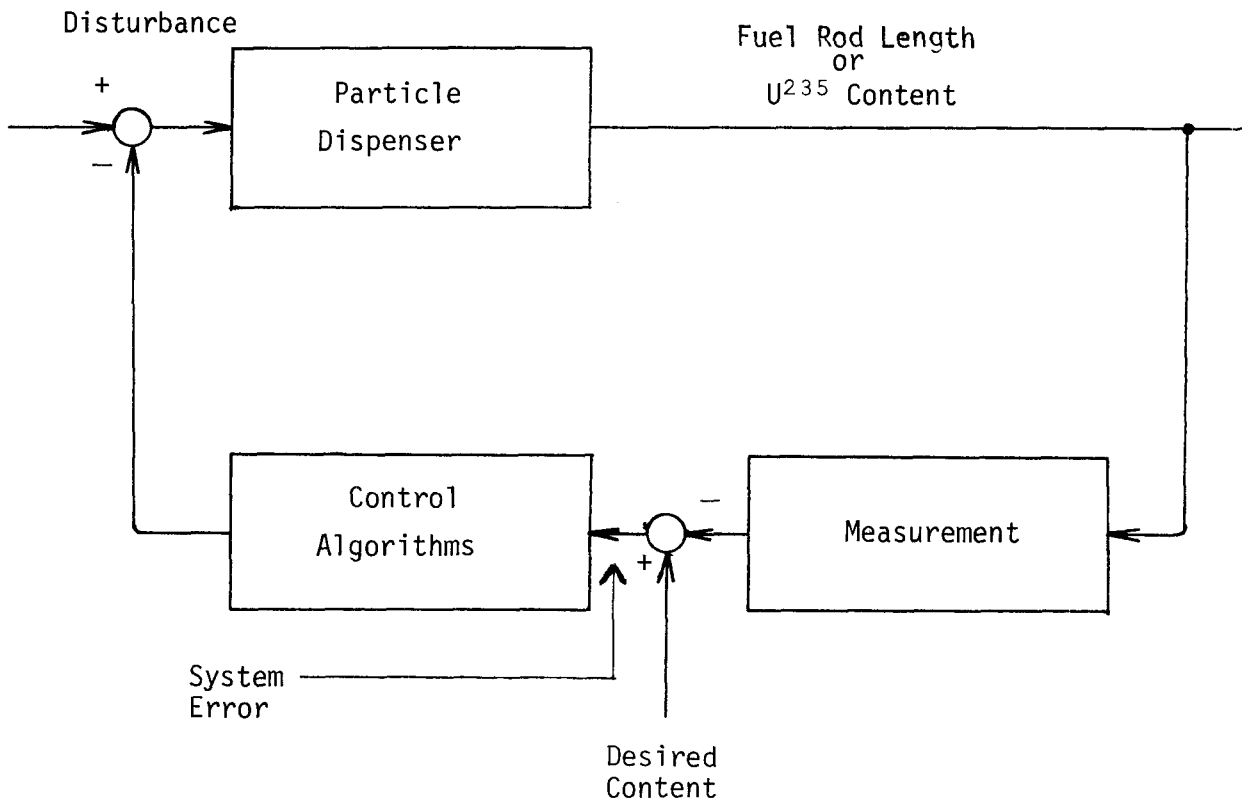


Fig. 16. Deterministic Block Diagram of the System.

Considering the desired fuel rod length as zero, the system differential equation becomes

$$\frac{dy(t)}{dt} + ay(t) = K_p x(t) - K_c y(t) . \quad (30)$$

Rearranging terms

$$\frac{dy(t)}{dt} + (a+K_c)y(t) = K_p x(t) . \quad (31)$$

For a process disturbance characterized by a linear function of the form

$$x(t) = K_d t ,$$

the process differential equation has the solution:

$$y(t) = K_p K_d \left[\frac{(a+K_c)t - (1-e^{-(a+K_c)t})}{(a+K_c)^2} \right] . \quad (32)$$

For a process in control, the disturbance $x(t)$ is a "slow" increase on drift with time and, hence, K_d is a small number. We can also adjust the controller gain K_c such that $K_c \gg a$ and $K_c + a \gg 1$. The process differential equation now becomes approximately

$$y(t) \cong K_p K_d \left[\frac{t}{K_c} \right] . \quad (33)$$

Since we have assumed a zero desired fuel rod length, $y(t)$ is now the system error which is essentially zero since $\frac{K_p}{K_c} \ll 1$. (We have tacitly assumed that this "drift" will not be maintained for a long period even with the uncertainty in the system parameters a , K_p , and K_d .)

Another control scheme is termed "proportional plus integral" or "PI" control and is characterized by the equation

$$e_c(t) = K_c \left[e(t) + b \int_0^t e(t) dt \right] . \quad (34)$$

The process differential equation becomes

$$\frac{dy(t)}{dt} + ay(t) = K_p x(t) - K_c \left[y(t) + b \int_0^t y(t) dt \right] . \quad (35)$$

Taking the first derivative of each side of the above equation and rearranging terms, we obtain

$$\frac{d^2y(t)}{dt^2} + (a+K_c) \frac{dy(t)}{dt} + bK_c y(t) = K_p \frac{dx(t)}{dt} . \quad (36)$$

Again assuming a disturbance of the form $x(t) = K_d t$, the response of the process differential equation becomes

$$y(t) = \frac{K_p K_d}{bK_c} \left[1 - \frac{bK_c}{\sqrt{bK_c - \left(\frac{a+K_c}{2}\right)^2}} e^{-\frac{(a+K_c)t}{2}} \sin\left(\sqrt{bK_c - \frac{(a+K_c)^2}{2}} t + \theta\right) \right] . \quad (37)$$

where

$$\theta = \tan^{-1} \left[\frac{bK_c - \left(\frac{a+K_c}{2}\right)^2}{bK_c} \right]$$

and

$$bK_c > \left(\frac{a+K_c}{2}\right)^2 .$$

To find the steady-state error e_{ss} , we allow time to approach infinity, or mathematically

$$e_{ss} = y_{ss} = \lim_{t \rightarrow \infty} y(t) = \frac{K_d}{bK_c} \quad (38)$$

Like the proportional controller, this steady-state error does not contain the system time constant "a". While this relationship does not require that the controller gain be much larger than the system time constant, the controller gain cannot be increased indefinitely without appropriately adjusting the controller parameter "b".

The controller constants are usually chosen by means of a Bode plot. To illustrate, we obtain the open loop transfer function (without feedback) of the process and controller in Laplace Transform notations as

$$\frac{y(s)}{x(s)} = \frac{K_p K_c [s+b]}{s[s+a]} \quad (39)$$

The Laplace variable "s" is now replaced with the imaginary quantity $j\omega$ to obtain

$$\frac{y}{x}(j\omega) = \frac{bK_p K_c}{a} \frac{1}{j\omega} \left[\frac{(1+j\frac{\omega}{b})}{(1+j\frac{\omega}{a})} \right] \quad (40)$$

For each value of ω this transfer function becomes a complex number with a magnitude and phase varying with ω . The magnitude of this transfer function becomes

$$\text{Mag.} \triangleq \frac{b}{a} \frac{bK_p K_c}{\omega} \left[\frac{\sqrt{1+(\frac{\omega}{b})^2}}{\sqrt{1+(\frac{\omega}{a})^2}} \right], \quad (41)$$

and the phase relationship

$$\phi \triangleq \tan^{-1}\left(\frac{\omega}{b}\right) - \tan^{-1}\left(\frac{\omega}{a}\right) - 90^\circ . \quad (42)$$

In the Bode plot these two quantities are plotted on semi-log paper. We plot decibels (abbreviated db) against $\log \omega$ rather than Mag against ω where

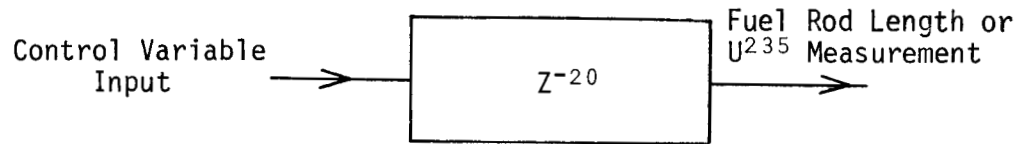
$$\text{decibel} \triangleq \text{db} \triangleq 20 \log(\text{Mag.}) \quad (43)$$

The characteristic to note from these Bode plots is the respective phase margins. Phase margin is defined as $180^\circ - \phi$ where ϕ is evaluated at the frequency ω where $\text{Mag} = 1.0$ (note that an absolute value of unity is equivalent to zero db). For systems such as the fuel rod length controller, a gain margin of 45° will allow an acceptable transient response while allowing some variation in " K_p " and " a " (a gain margin of zero degrees produces an unstable system).

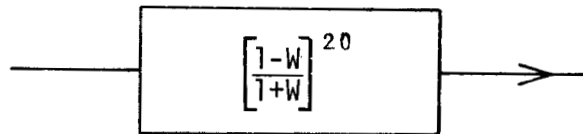
With these preliminary remarks we now recognize that the system is truly discrete in nature and, thus, make use of the Z transform. The backward operator B of Box and Jenkins is related to this Z transform variable by

$$Z^{-1} = B . \quad (44)$$

The Fuel Rod Fabrication system of Fig. 1 consisting of a 20-sample delay between control variable input and the measurement of fuel rod length can be expressed in transfer function form as shown in Fig. 17a.



a) Transfer Function In The "Z" Notation



b) Transfer Function In The "W" Notation

Fig. 17. Open Loop Transfer Function of the System.

We now make the transformation

$$Z = \frac{1+W}{1-W} \quad (45)$$

where W is a complex parameter

$$W = U + jv . \quad (46)$$

This transformation plots the interior of the unit circle in the "Z" domain into the left-hand portion of the "W" domain. If the real portion of the W variable is zero,

$$Z = \frac{1 + jv}{1 - jv} . \quad (47)$$

With this transformation, we can now utilize the Bode plot. The relationship between the variable "v" and frequency ω in radians per second then becomes

$$\omega = 2 \tan^{-1}(v) . \quad (48)$$

The open loop block diagram in the " ω " domain is shown in Fig. 17b. The Bode plots for the open loop system and the compensation (control algorithm) are shown in Fig. 18. In general, proportional control is not suitable for a system consisting of pure time delays as illustrated in Fig. 19. The constant magnitude and increasing phase lag limit the allowable low frequency gain of the system and, hence, the steady-state error.

To obtain the desired phase margin of 45° , the controller transfer function must be

$$G_c(jv) = \frac{K}{\frac{Jv}{b} 1 + J\frac{v}{a}} \quad (49)$$

where

$$K = 8$$

$$a = 0.01$$

$$b = 0.001.$$

Performing the inverse W transformation, the compensation algorithm becomes

$$G_c(Z) = \frac{79 \times 10^{-6} [Z^2 + 2Z + 1]}{[Z^2 - 1.980148Z + 0.98019802]} . \quad (50)$$

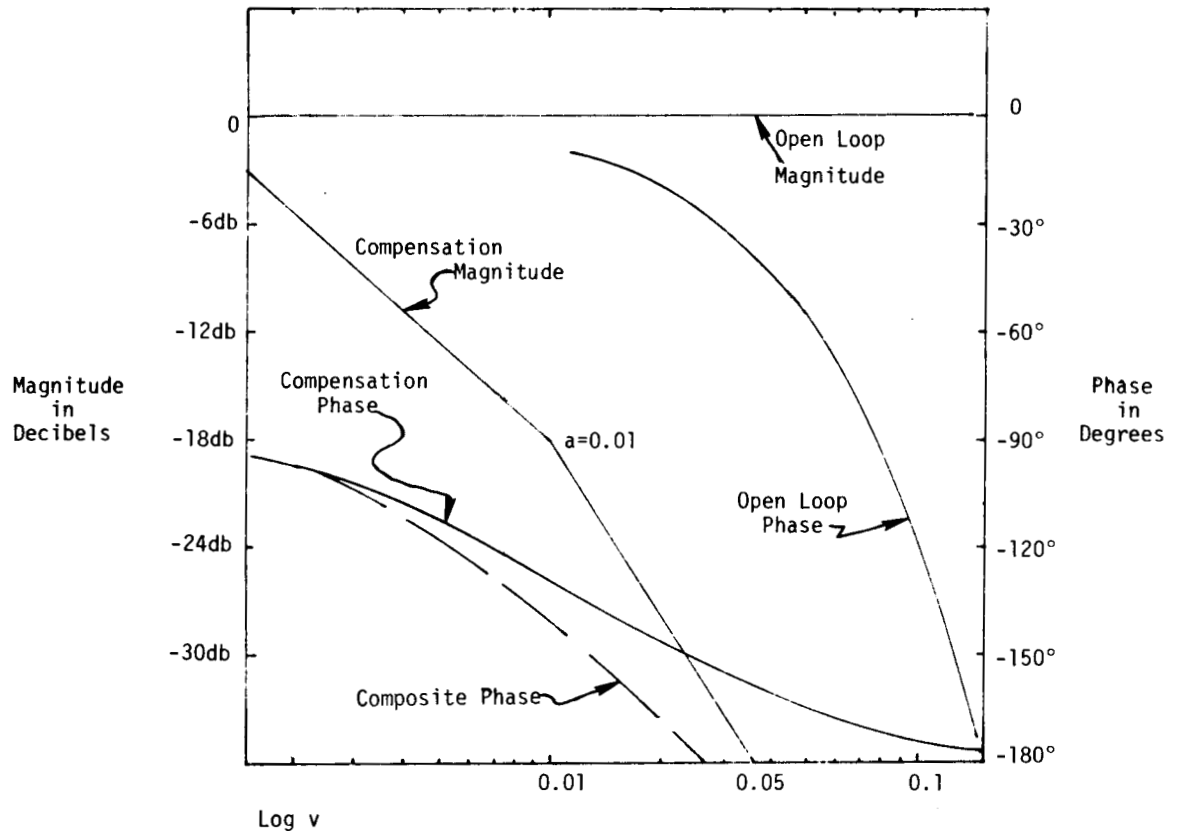


Fig. 18. The Bode Plot.

The system was simulated using IBM's Continuous System Modeling Program (CSMP). The simulation diagram is shown in Fig. 20, and the actual program is indicated in Appendix A. In the notation of Box and Jenkins, the linear filter characterizes the noise process as

$$[1 - 0.237B - 0.086B^2 - 0.189B^3 - 0.158B^4]N_t = a_t \quad (51)$$

where

$$N_t = P_t$$

$$a_t = E_1 .$$

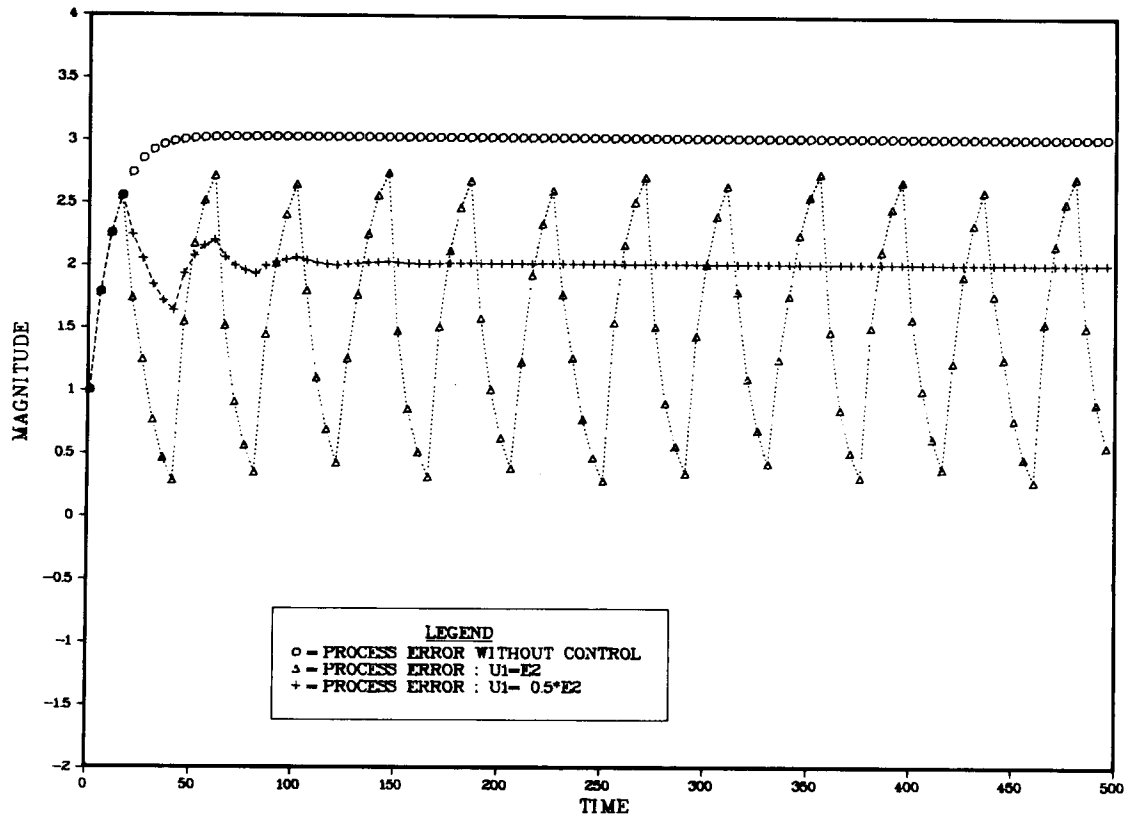


Fig. 19. Step Function Response For Proportional Control.

The step function response of the system is shown in Fig. 21. It is seen that the closed loop system is stable. The process error will eventually be driven to a zero value. While more sophisticated algorithms could be derived to improve the transient response, they will all be limited by the type of transfer function characterizing this system.

The Box-Jenkins algorithm was also simulated as shown in Fig. 22.

In their notation

$$L_1^{-1}(B) = 1$$

$$L_2(B) = 1$$

$$f = 19$$

$$N_t = 1 + \sum_{i=1}^{\infty} \psi_i B^i a_t . \quad (52)$$

We have chosen to truncate the infinite series to 40 terms. Thus, the algorithm becomes

$$\frac{L_3}{L_4}(B) = \frac{\psi_{20} + \psi_{21}B + \dots + \psi_{30}B^{10} + \dots + \psi_{40}B^{20}}{1 + \psi_1 B + \psi_2 B^2 + \dots + \psi_{19} B^{19}} . \quad (53)$$

In the simulation diagram we utilize the standard control theory representation

$$B = Z^{-1} . \quad (54)$$

The step function response is now shown in Fig. 23.

In comparing the two design approaches, it is seen that both designs insure a stable system. For a deterministic upset, the classical design system will eventually obtain a zero process error as compared to a reduction of 4% for the Box-Jenkins system. However, the Box-Jenkins filter is designed to minimize the output mean square error; with

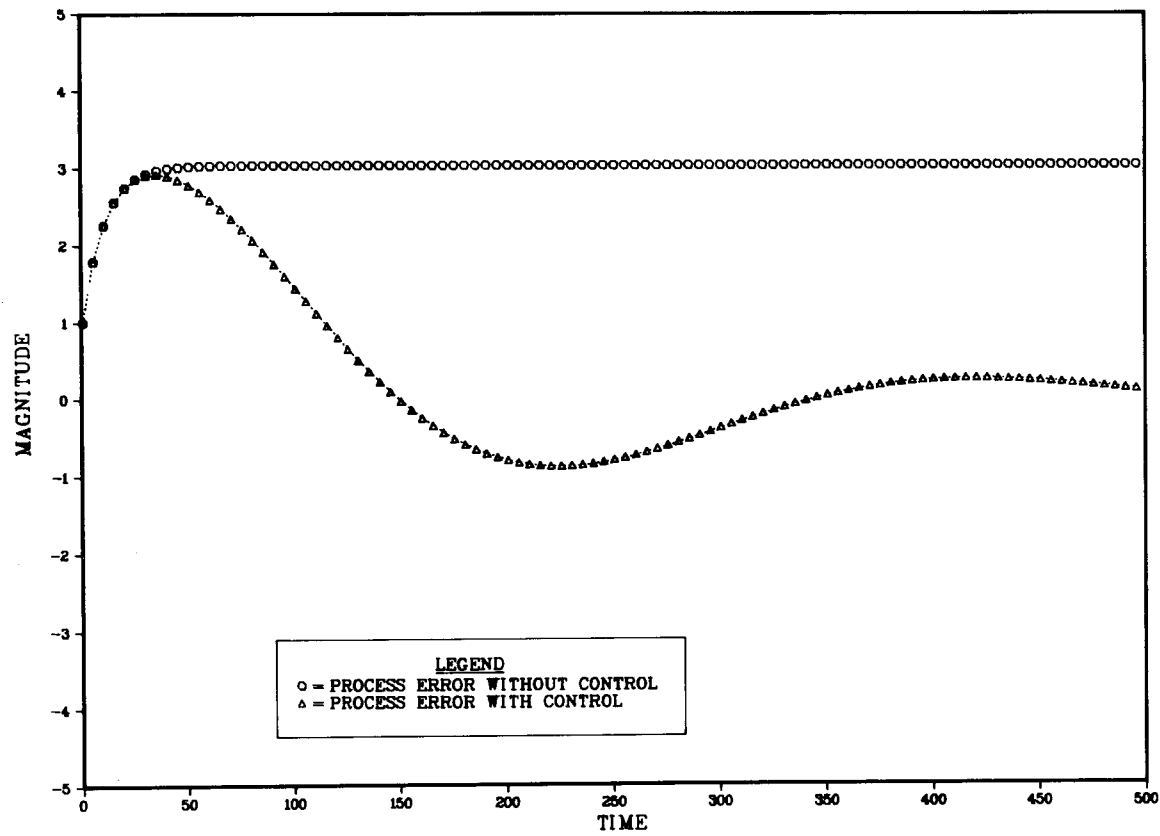


Fig. 21. Step Function Response For the Classical Design.

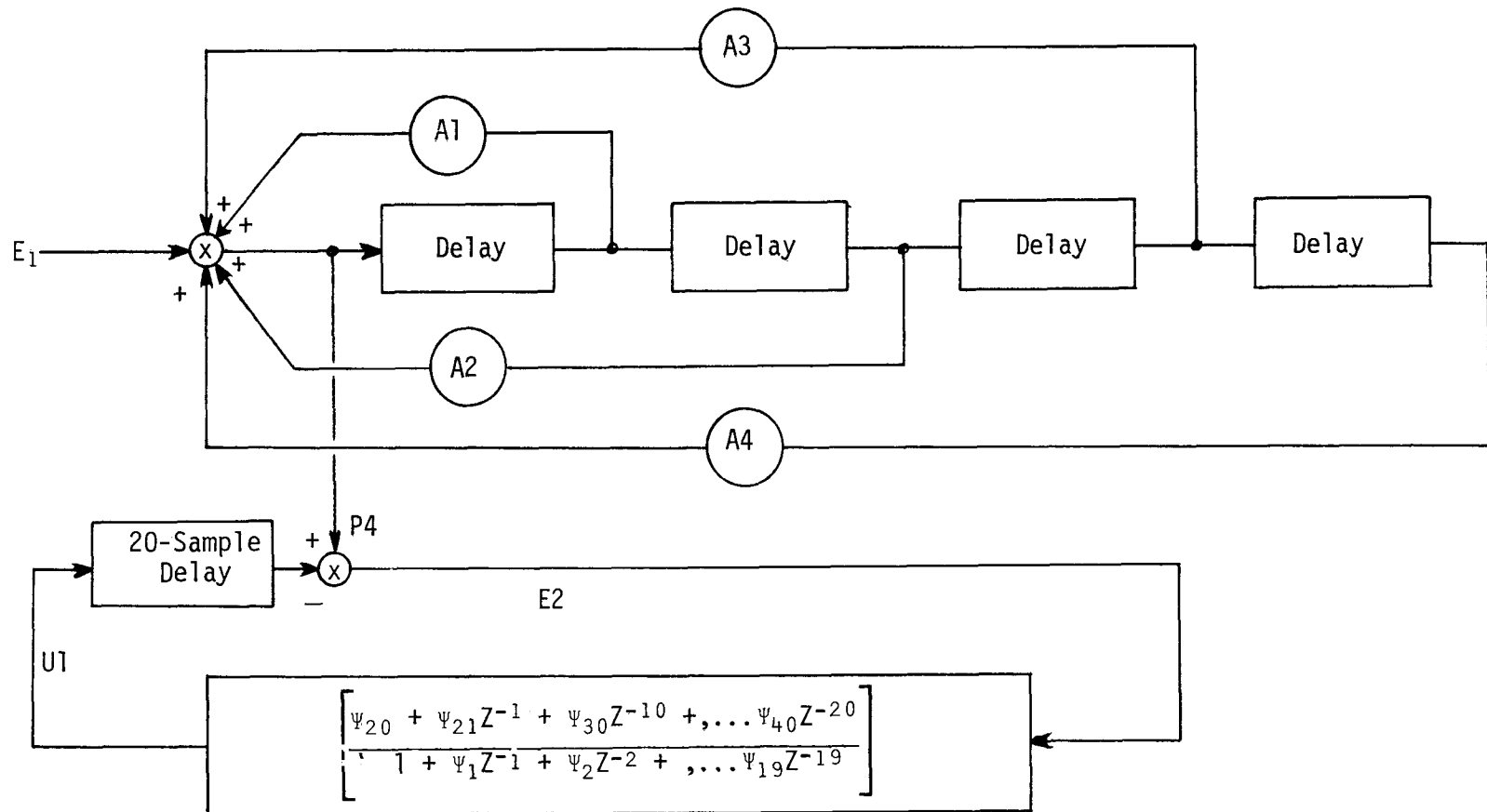


Fig. 22. Simulation Diagram (Box-Jenkins Design).

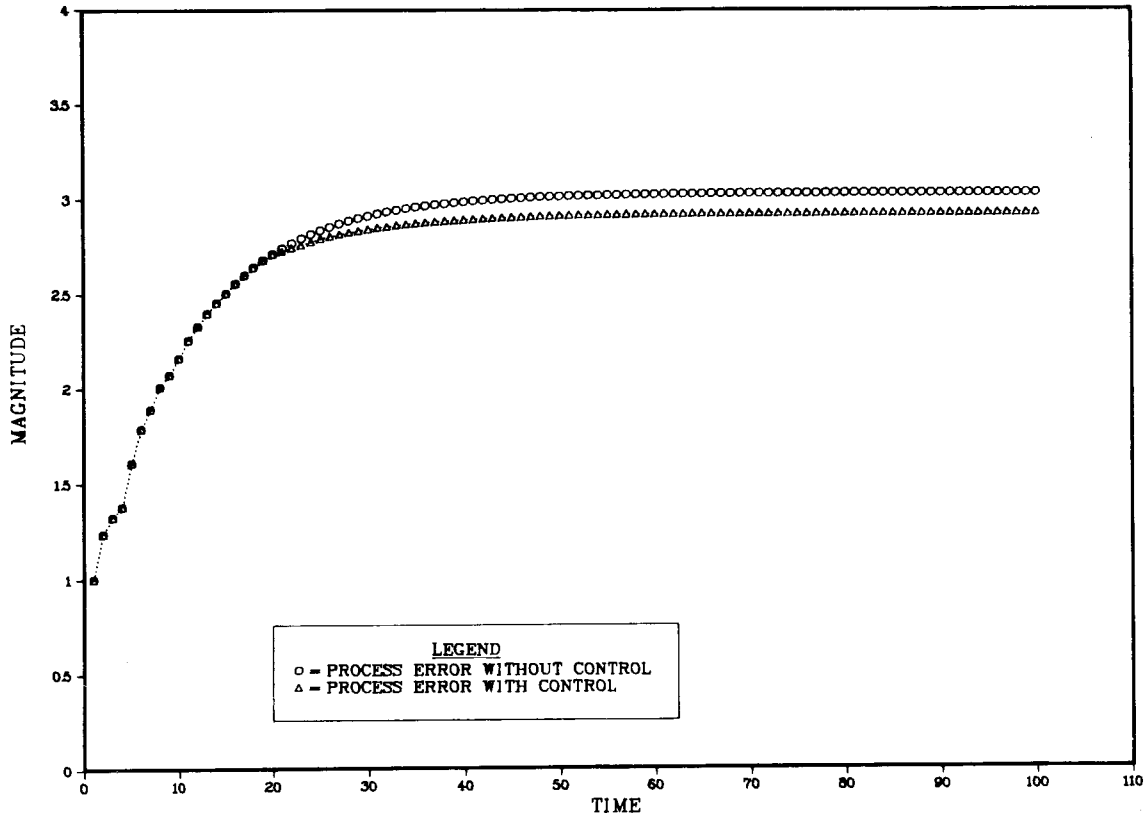


Fig. 23. Step Function Response For the Box-Jenkins Design.

the large number of delays in the system, one would intuitively expect a "sluggish" control system.

The applicability of the Box-Jenkins approach depends upon the ability to determine a discrete time model which neither varies over time nor with different campaigns. If such a model cannot be found, the Box-Jenkins approach should not be used. The classical design approach is rather insensitive to process model and campaign. The magnitude of gains can be adjusted by trial and error to achieve satisfactory control. The independence of the classical design approach from the process model and campaigns makes it a viable candidate for the control mechanism used.

VI. OTHER QUALITY CONTROL METHODS

The previous methods were devised to control the process by automatic feedback. Other methods are available to detect shifts in process characteristics. Two of these are the Shewhart control chart and the CUSUM control chart. These methods provide no automatic feedback into the system, but they can give early warning so that adjustments can be made. The general theory surrounding control charts is based on the assumption that the variations (or departures from target) of quality are random. If these random variations are observed across time, they will show no cycles or runs or any other defined pattern. The conditions which produced this chance variation are said to be "under control". They are under control in the sense that, if chance causes are alone at work, then the amount and character of the variation may be predicted for large numbers, and it is not possible to trace the variation of a specific instance to a particular cause. If variations in the data follow some

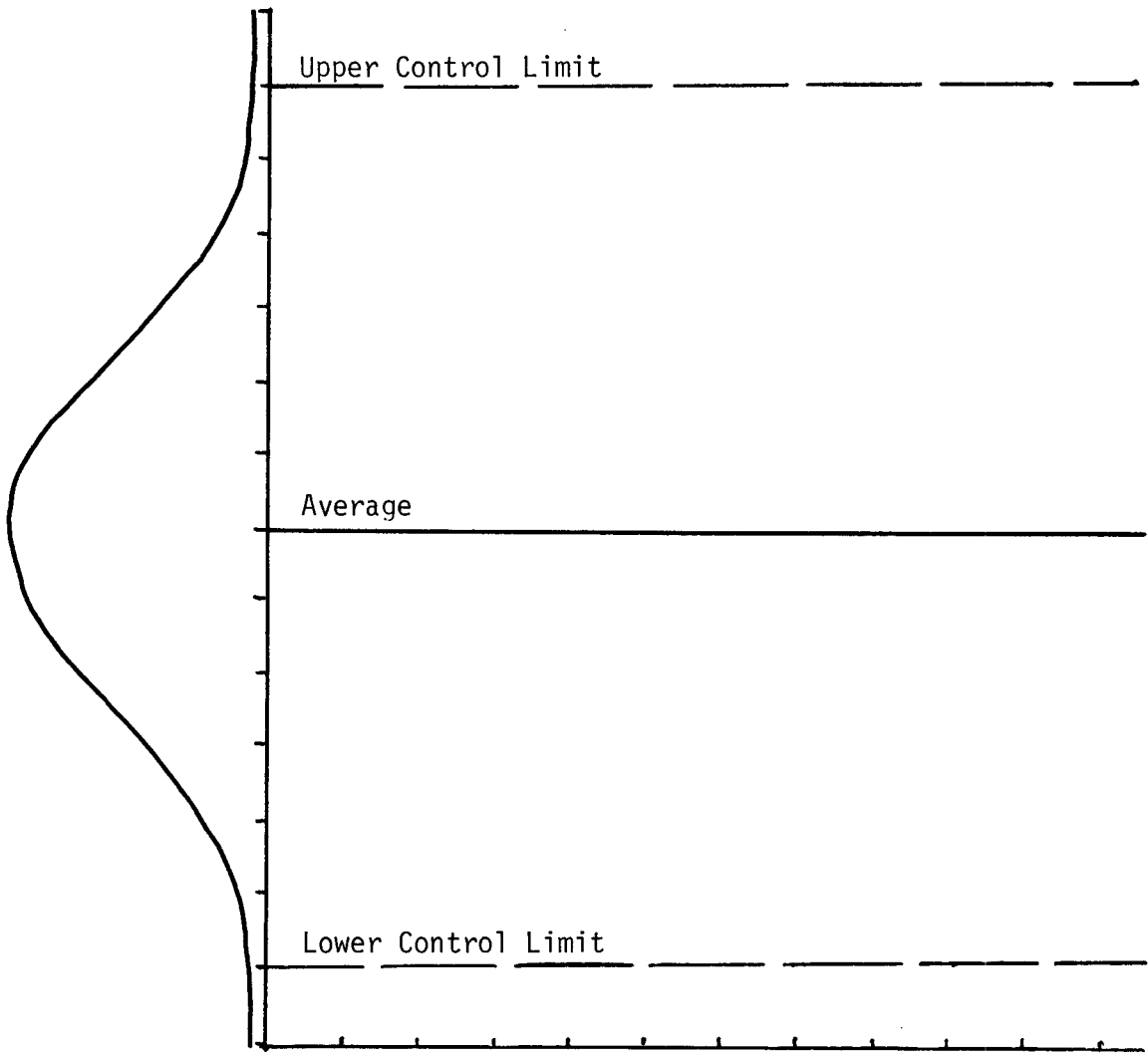
defined pattern (e.g., increasing or decreasing with time), then it is concluded that one or more assignable causes are at work. In this case the conditions producing the variation are said to be "out of control".

Suppose samples of a given size are taken from a process at regular intervals and some statistic, x , is computed. This might be the sample mean, percent defective, or sample range. Being a sample result, x will be subject to sampling fluctuations. If only random variations are present, the sampling fluctuations in x will be distributed in a definite statistical pattern such as that pictured in Fig. 24. This sampling distribution describes the probability that x lies in some interval. If enough samples are taken, it is possible to estimate the mean and certain extreme points of this distribution. Often we can assume that the sampling distribution of x is normal. In this case we can estimate the mean of x from the mean of the samples. Also, the within-sample variation can be used to estimate the standard deviation of x . Using these two estimates, we can determine probability points. For example, the points U and L marked on Fig. 24 might indicate the upper (U) and lower (L) 0.001 probability points. That is, only one in a thousand samples will exceed the upper (or lower) point if only chance variations are at work. If we take Fig. 24 and rotate it 90° , extend horizontal lines through the estimated mean of x and through an extreme value on the upper and lower tail of the distribution of x (see Fig. 25), the result is a control chart for x .

If sample values of x are plotted on the control chart and they remain within the control limits with no nonrandom runs up or down, then it can be said that the process is in statistical control at the designated level with respect to the given measure of quality.



Fig. 24. Distribution of Chance Variations (x) in a Sample Measure of Quality.



Time Order of Production

Fig. 25. Control Chart for x .

The control limits shown in Fig. 25 are 0.001 probability limits. If a sample falls outside these limits, then a search is begun for an assignable cause. The probability that such a search is performed when chance causes are at work is the sum of the upper and lower probability limits. In the example this is 0.002 or 2 out of a thousand. Thus, if a point falls outside the control limits, there is little chance that it occurred by random fluctuations.

Control limits can also be chosen as multiples of the standard deviation, σ . If the probability distribution is normal, then the 0.001 probability limits are practically equivalent to 3σ limits; for under a normal curve, the probability that the deviation from the mean will exceed 3σ in one direction is 0.00135. Generally, the 3σ limit is used with a 2σ limit incorporated as a warning limit. Briefly, the following scheme is generally employed:

<u>Event</u>	<u>Action</u>
Deviation from target less than 2σ .	None—process is in control.
One observation deviates from target by 2σ , but less than 3σ .	Watch process closely—indication of nonrandom behavior.
Two observations, in succession, deviate from target by 2σ .	Stop process—search for an assignable cause.
One observation deviates from target by 3σ .	Stop process—search for an assignable cause.

Alternatively, control limits can be set by management. The limits set by management impose the type of quality that is acceptable and may be wider or narrower than the standard 3σ limits. Regardless of how the control limits are formed, the above "event-action" scenario is applicable.

Attempts to run together the information from several successive results have resulted in charts based on some form of weighted mean of

past results. In particular, the Arithmetic Running Mean has been used in some instances. The mean of the last K results is calculated and plotted. When a new result is obtained, the mean of the most recent K results is redetermined and plotted. Lack of control is indicated by the running mean falling outside a single control limit.

The Geometric Mean chart (also called an Exponentially Weighted Mean) uses weights which get progressively smaller as the results become more distant in time. The weights change progressively by the factor " $1-R$ " ($R < 1$). In this form, lack of control is indicated by the geometric mean falling outside a single control limit.

Another type of control chart is the CUSUM control chart. The name CUSUM comes from the fact that what is plotted in this control chart is the cumulative sum. Its advantage over the Shewhart control chart is that it will detect sudden and persistent change in the process average more rapidly than a comparable Shewhart chart. The Shewhart chart is more effective at picking up single large changes in the process.

The Cumulative Sum chart (CUSUM) plots at time t (or for the t^{th} sample) the statistic

$$\begin{aligned}
 S(t) &= \sum_{i=1}^t (\text{Observed Sample Value at time } i - \text{Target Value}) \\
 &= \sum_{i=1}^t (x_i - k) .
 \end{aligned} \tag{55}$$

Thus, it cumulates the deviations from target. If chance causes are producing the deviations, then some of them will be positive and some negative, thus canceling each other, and $S(t)$ will remain near zero. On the other

hand, if assignable causes are in effect, these may cause trends up (or down) which will tend to keep the deviations consistently positive (or negative) and, thus, increasing $S(t)$ in magnitude. Typically, the CUSUM chart looks like the Shewhart control chart, but the upper and lower limits are constructed differently.

For the CUSUM chart, the easiest form of test is one in which the chart goes in one direction at good quality (say downwards) and in the opposite direction at bad quality. On this type of chart, the mean value corresponding to zero slope is generally called the reference value. A rise from the lowest point of the chart, by more than some known amount, h , called the decision interval, provides the criterion for a change. Algebraically, if the reference value is k and the decision interval is h , a decision that a change has taken place is made if $\sum_{i=n-r+1}^n (x_i - k) \geq h$; where r is any integer less than or equal to n .

If we wish to detect changes in either direction with a CUSUM chart, a simple two-sided test is required, and a V-mask is employed. This is equivalent to the simultaneous application of two of the one-sided tests described above. The V-mask and its parameters are shown in Fig. 26. The relationship between the V-mask parameters (half-angle = θ and lead distance = d horizontal plotting intervals) and the reference value (k) and decision interval (h) used in the one-sided test is

$$k = \omega \tan \theta , \quad (56)$$

and

$$h = \omega d \tan \theta , \quad (57)$$

where ω equals vertical scale distance per horizontal plotting interval (called the scale factor).

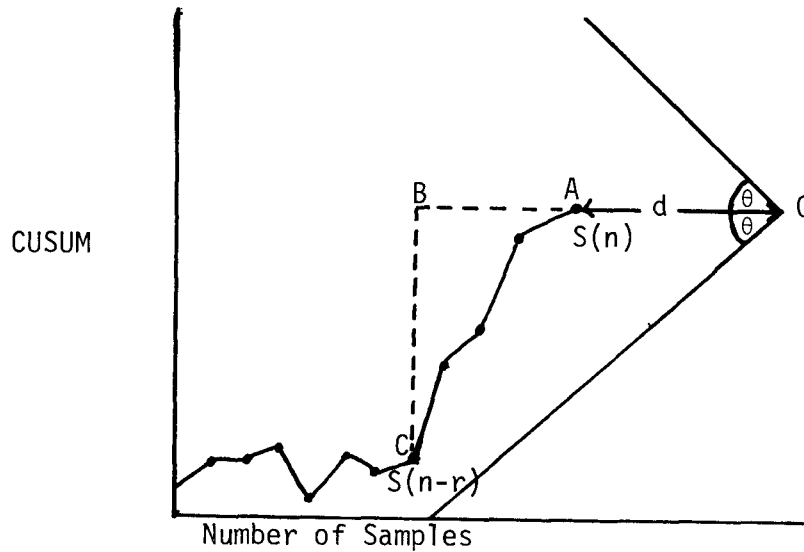


Fig. 26. Cumulative Sum of $(x_i - k)$ Plotted Against Number of Samples Using a V-mask.

Figure 26 shows a mask with limbs inclined at an angle θ to the horizontal. The cumulative sum at A, which is the last plotted point, is $S(n)$ and at C is $S(n-r)$. The point O is the vertex of the V-mask.

Extend OA and let the perpendicular from C meet it at B. Then,

$$CB = S(n) - S(n-r) \quad (58)$$

$$BA = r\omega \quad (59)$$

The path of the plotted points will cross the lower limb of the V when

$$BC \geq BO \tan \theta, \quad (60)$$

that is, when

$$[S(n) - S(n-r)]/\omega \geq (r+d) \tan \theta \quad (61)$$

or

$$\sum_{i=n-r+1}^n (x_i - \omega \tan \theta) \geq \omega d \tan \theta . \quad (62)$$

This is equivalent to cumulating deviations of x_i from a reference value $k = \omega \tan \theta$ and using a decision interval $h = \omega d \tan \theta$.

This decision procedure implies an initial choice of an Acceptable Quality Level (A.Q.L.), which would have an average slope less than that of the limb of the V-mask, and of a Rejectable Quality Level (R.Q.L.), which would have an average slope steeper than the V-mask. Definition of these two quality levels and the length of time at each level before reaching a decision will define a unique optimum decision scheme. The expected length of time until detection is called the Average Run Length (ARL). A nomogram from which ARL values can be calculated when x_i is normally distributed can be found in a paper by Kemp [3].

In summary, the advantages of CUSUM charts over Shewhart control charts are:

- 1) Changes in mean level can be detected visually by a change in slope of the chart.
- 2) The point of change can be located visually.
- 3) Changes of between 0.5σ and 2.0σ are detected about twice as quickly using the CUSUM. Alternatively, the change can be detected at the same time, but with smaller samples.

The advantages of the Shewhart control chart over the CUSUM are:

- 1) The Shewhart control chart is extremely simple to set up.
- 2) If only large deviations in the process ($>2\sigma$) are of concern, then the Shewhart chart will detect it faster than the CUSUM.

An example will help clarify the previous methods. In addition to the CUSUM and Shewhart control charts, we shall include the Kalman Filter. For this example we assume that the variance of the process is known and equal to unity. The process will be declared out of control if two consecutive points exceed the two-sigma limits or if one point exceeds the three-sigma limits. Thus, for the Shewhart control chart we examine $x(t)$, the observation at time t . If μ denotes the target value and σ denotes the process standard deviation, then we declare the process out of control at time t if

$$|x(t-1)-\mu| > 2\sigma \quad \text{and} \quad |x(t)-\mu| > 2\sigma$$

or

$$|x(t)-\mu| > 3\sigma .$$

Since we have chosen $\sigma=1$ for convenience, the above inequalities reduce to

$$|x(t-1)-\mu| > 2 \quad \text{and} \quad |x(t)-\mu| > 2$$

or

$$|x(t)-\mu| > 3 .$$

Given that σ is known, the CUSUM can be set up in a manner similar to the Shewhart control chart. Two- and three-sigma limits for the CUSUM can be calculated using

$$\begin{aligned}
\text{Var}(S(t)) &= \text{Var} \sum_{i=1}^t x(i) \\
&= \sum_{i=1}^t \text{Var}(x(i)) + 2 \sum_{i=1}^{t-1} \sum_{\substack{j=2 \\ i < j}}^t \text{Cov}(x(i), x(j)) . \quad (63)
\end{aligned}$$

Since the measurements are assumed independent, then the covariance will be zero, and the variance of $S(t)$ is

$$\begin{aligned}
\text{Var}(S(t)) &= \sum_{i=1}^t \text{Var}(x(i)) \\
&= \sum_{i=1}^t \sigma^2 \\
&= t\sigma^2 . \quad (64)
\end{aligned}$$

Instead of using the CUSUM directly, we shall use the average CUSUM (ACUSUM) defined by

$$A(t) = S(t)/t = \sum_{i=1}^t x(i)/t . \quad (65)$$

The variance of $A(t)$ is

$$\text{Var}(A(t)) = \frac{1}{t^2} \text{Var}(S(t)) = \frac{\sigma^2}{t} . \quad (66)$$

Thus, the variance of $A(t)$ decreases with time—this is in contrast with the Shewhart control chart where the variance remains constant over time. The process is said to be out of control at time t by the ACUSUM chart if

$$|A(t-1) - \mu| > \frac{2\sigma}{\sqrt{t-1}} \quad \text{and} \quad |A(t) - \mu| > \frac{2\sigma}{\sqrt{t}}$$

or

$$|A(t) - \mu| > \frac{3\sigma}{\sqrt{t}} .$$

As a basis of comparison, the Kalman Filter is performed sequentially as follows:

- 1) Initialization: $\mu(0) = Y(0)$, $G(0) = \sigma^2 = 1$
- 2) Gain: $k(t) = G(t-1)/[G(t-1) + \sigma^2] = G(t-1)/[G(t-1) + 1]$
- 3) State Update: $\mu(t) = \mu(t-1) + k(t)[x(t) - \mu(t-1)]$
- 4) Error variance for (t): $G(t) = \frac{\sigma^2 G(t-1)}{G(t-1) + \sigma^2} = \frac{G(t-1)}{G(t-1) + 1}$

Steps 2-4 are repeated after receipt of each observation. The Kalman Filter declares the process out of control if

$$|\mu(t-1) - \mu| > 2\sqrt{G(t-1)} \quad \text{and} \quad |\mu(t) - \mu| > 2\sqrt{G(t)}$$

or

$$|\mu(t) - \mu| > 3\sqrt{G(t)} .$$

The following 20 numbers were randomly selected from a normal population with variance equal to 1. The first 10 numbers have a true mean value $\mu=10$ while the last 10 have a true mean value equal to 9. The value $\mu=10$ is considered to be the target value. The process has a step change at time $t=11$ to a new mean level of 9. It is this change in the process that we wish to detect.

t =	1	2	3	4	5	6	7	8	9	10	11	12	13	14	15	16	17	18	19	20
x(t) =	8.9	10.1	8.8	10.2	10.9	10.8	7.9	9.8	8.9	10.4	7.9	8.3	10.0	9.3	8.0	11.3	8.6	7.5	8.7	10.8

Table 6 shows that the Shewhart control chart technique does not detect the change in level over the time span while both the Kalman Filter and the ACUSUM detect it by period 15.

ORNL-DWG 79-7705

Table 6. Comparison of Control Chart Methods.

Time	SHEWHART		ACUSUM		KALMAN FILTER	
	$x(t)-\mu$	Two Sigma Limits	$A(t)-\mu$	Two Sigma Limits	$\mu(t)-\mu$	Two Sigma Limits ($2\sqrt{\hat{\sigma}^2(t)}$)
1	-1.1	2	-1.10	2.00	-0.55	1.41
2	0.1	2	-0.50	1.41	-0.33	1.15
3	-1.2	2	-0.73	1.15	-0.55	1.00
4	0.2	2	-0.50	1.00	-0.40	0.89
5	0.9	2	-0.22	0.89	-0.18	0.82
6	0.8	2	-0.05	0.82	-0.04	0.76
7	-2.1*	2	-0.34	0.76	-0.30	0.71
8	-0.2	2	-0.33	0.71	-0.29	0.67
9	-1.1	2	-0.41	0.67	-0.37	0.63
10	0.4	2	-0.33	0.63	-0.30	0.60
11	-2.1*	2	-0.49	0.60	-0.45	0.58
12	-1.7	2	-0.59*	0.58	-0.55	0.55
13	0.0	2	-0.546	0.555	-0.51	0.54
14	-0.7	2	-0.56*	0.53	-0.520*	0.52
15	-2.0*	2	-0.65*†	0.52	-0.61*†	0.50
16	1.3	2	-0.53*	0.50	-0.50*	0.49
17	-1.4	2	-0.58*	0.49	-0.55*	0.47
18	-2.5*	2	-0.69*	0.47	-0.65*	0.46
19	-1.3	2	-0.72*	0.46	-0.69*	0.45
20	0.8	2	-0.65*	0.45	-0.61*	0.44

* Outside of control limits

† Process said to be out of control at this time

SUMMARY

Several results were obtained in this report. In summarizing the report, a difficulty appears since no one method was always better than another; rather, for certain situations one method did better, but for another situation a different method was best. This indicates that perhaps more than one method should be employed to give the best results possible.

The following shows the areas this report discussed and the methods compared:

I. Process Measurement and Detection of Shift in Level	<ul style="list-style-type: none"> { Kalman Filter { Weighted Least Squares { Shewhart Control Chart
II. Process Control	<ul style="list-style-type: none"> { Box-Jenkins { Classical Design { Shewhart Control Chart { Cumulative Sum Chart

Under I, it is our view that the Kalman Filter does the best job overall. The reasons for this are: (1) information about the system can be incorporated into the system model improving detection; (2) assumptions as to whether the process has a linear drift or whether it changes by a series of jumps is not important; (3) it yields a minimum variance unbiased estimator of the process level, and (4) it can supply a good estimate of the process level to use in feedback control. Again, it should be pointed out that if the process is known to drift in a linear fashion, then weighted linear least squares may be better.

Under II, the Box-Jenkins methods appear too sensitive to be applicable to fuel rod production. The classical design obviates the problems found using the Box-Jenkins procedures and is the recommended choice if dynamic (i.e., continuous) control is desired. In the case where continuous control of the process is not necessary (for example, a process that drifts very slowly over time), then either the Shewhart control chart or the CUSUM are the methods of choice. Again, this author feels that the CUSUM (or ACUSUM) is better in most cases. The Shewhart control chart is effective for large jumps because the observations are not averaged or lumped together, but it is extremely poor for slow drifts. The simplicity of these procedures certainly makes them attractive and using both in tandem would present no problems.

Incorporating both I and II together, the choice would be the Kalman Filter and the classical control theory if continuous control is desired. If continuous control is not important, then the Kalman Filter can be used as a control charting device itself, and it has been shown to be as sensitive or more sensitive than the CUSUM or Shewhart control charts (see [4]) for detecting material losses.

REFERENCES

1. G.E.P. Box and G. M. Jenkins, "Time Series Analysis Forecasting and Control", Holden-Day, 1970.
2. L. H. Tee and S. M. Wu, "An Application of Stochastic and Dynamic Models For the Control of a Papermaking Process", *Technometrics*, 19:2, pp. 481-496, 1972.
3. Kenneth W. Kemp, "The Use of Cumulative Sums for Sampling Inspection Schemes", *Applied Statistics*, Vol. XI, p. 20, 1962.
4. D. H. Pike, G. W. Morrison, and D. J. Downing, "Time Series Analysis Techniques Applicable to Nuclear Material Accountability Data," NUREG/CR-0374 (ORNL/NUREG/CSD-10), 1978.

APPENDIX A

CSMP PROGRAM TO GENERATE STEP FUNCTION RESPONSE
FOR THE BOX-JENKINS DESIGN

ORNL-DWG 79-7709

```
INITIAL
PARAM A1=0.237,A2=0.086,A3=0.189,A4=.158,B=.001,SAMTIM=1.0,T=1.0
PARAM C5=1.C,C7=0.0
B1=0.237
E2=0.14217
B3=0.24308
E4=0.27263
B5=0.14983
E6=0.12736
B7=0.133
E8=0.11387
B9=0.08614
E10=0.07548
B11=0.06788
E12=0.05684
B13=0.04719
E14=0.04082
B15=0.03519
E16=0.02975
B17=0.02525
E18=0.02164
B19=0.01848
E20=0.01571
B21=0.01339
E22=0.01144
B23=0.00975
E24=0.00831
B25=0.00709
E26=0.00604
B27=0.00515
E28=0.00439
B29=0.00375
E30=0.00319
B31=0.00272
E32=0.00232
B33=0.00198
E34=0.00169
B35=0.00144
E36=0.00123
B37=0.00105
E38=0.00089
B39=0.00076
E40=0.00065
```

```
Z1=0.0
Z2=0.0
Z3=0.0
Z4=0.0
Z5=0.0
Z6=0.0
Z7=0.0
Z8=0.0
Z9=0.0
Z10=0.0
Z11=0.0
Z12=0.0
Z13=0.0
Z14=0.0
Z15=0.0
Z16=0.0
Z17=0.0
Z18=0.0
Z19=0.0
E3=0.0
E4=0.0
E5=0.0
E6=0.0
E7=0.0
E9=0.0
E10=0.0
E11=0.0
E12=0.0
E13=0.0
E14=0.0
E15=0.0
E16=0.0
E17=0.0
E18=0.0
E19=0.0
E20=0.0
E21=0.0
E22=0.0
DYNAMIC
E1=STEP(0.0)
TX=IMPULS(0.0,SAMTIM)
EZ=TX*E1
X1=DELAY(100,SAMTIM,EZ)
X2=DELAY(100,SAMTIM,X1)
X3=DELAY(100,SAMTIM,X2)
X4=DELAY(100,SAMTIM,X3)
P1=DELAY(100,SAMTIM,P2)
P4=EZ-A1*X1-A2*X2-A3*X3-A4*X4
```

```

PROCEDURE E2,U1=BOX(P4)
E2=P4-Y20
U1=-B1*Z1-B2*Z2-B3*Z3-B4*Z4-B5*Z5-B6*Z6-B7*Z7-B8*Z8-B9*Z1 ...
-B10*Z10-B11*Z11-E12*Z12-B13*Z13-B14*Z14-B16*Z16-B17*Z17 ...
-E18*Z18-B19*Z19+B21*E3+B22*E4+B23*E5+B24*E6+B25*E7+B26*E8 ...
+E27*E9+E28*E10+B29*E11+B30*E12+B31*E13+B32*E14+E33*E15 ...
+E34*E16+E35*E17+B36*E18+B37*E19+B38*E20+B39*E21+B40*E22
Z19=Z18
Z18=Z17
Z17=Z16
Z16=Z15
Z15=Z14
Z14=Z13
Z13=Z12
Z12=Z11
Z11=Z10
Z10=Z9
Z9=Z8
Z8=Z7
Z7=Z6
Z6=Z5
Z5=Z4
Z4=Z3
Z3=Z2
Z2=Z1
Z1=U1
E22=E21
E21=E20
E20=E19
E19=E18
E18=E17
E17=E16
E16=E15
E15=E14
E14=E13
E13=E12
E12=E11
E11=E10
E10=E9
E9=E8
E8=E7
E7=E6
E6=E5
E5=E4
E4=E3
E3=E2
Y20=DELAY(20,20.0,U1)
ENDPRO
PRTPLT U1,E2
TIMER FINTIM=1000.,OUTDEL=10.0,DELT=1.0
LABEL CR. BAILEY FOR
END
STOP
ENDJOB

```

CSMP PROGRAM TO GENERATE STEP FUNCTION RESPONSE
FOR THE CLASSICAL DESIGN

ORNL-DWG 79-7695

```

INITIAL
PARAM A1=0.237,A2=0.086,A3=0.189,A4=.158,B=.001,SAMTIM=1.0,T=1.0
PARAM C5=1.C,C7=0.0
P2=0.0
Y20=0.0
P1=0.0
DYNAMIC
E1=1.0
TX=IMPUIS(0.0,SAMTIM)
EZ=TX*E1
X1=DELAY(100,SAMTIM,P4)
X2=DELAY(100,SAMTIM,X1)
X3=DELAY(100,SAMTIM,X2)
X4=DELAY(100,SAMTIM,X3)
P4=EZ+A1*X1+A2*X2+A3*X3+A4*X4
PROCEDURE Y20,E2,P3,U1=DUMMY(P4)
E2=P4-Y20
P3=E2+1.980198*P2-.98019802*P1
U1=E2
Y20=DELAY(20,20.,U1)
P1=P2
P2=P3
ENDPRO
PRTPLT E2,P4
TIMER FINTIM=500.,OUTDEL=10.,DELT=1.0
LABEL CR. BAILEY FOR
END
STOP
ENDJOB

```

CSMP PROGRAM TO GENERATE STEP FUNCTION RESPONSE
FOR THE PROPORTIONAL CONTROL

ORNL-DWG 79-7701

```

INITIAL
PARAM A1=0.237,A2=0.086,A3=0.189,A4=.158,B=.001,SAMTIM=1.0,T=1.0
PARAM C5=1.C,C7=0.0
E1=0.237
E2=0.14217
E3=0.24308
E4=0.27263
E5=C.14983
E6=0.12736
E7=0.133
E8=0.11387
E9=0.08614
E10=0.07548
E11=0.06788
E12=0.05684
E13=0.04719
E14=0.04082
E15=0.03519
E16=0.02975
E17=0.02525
E18=0.02164
E19=0.01848
E20=0.01571
E21=0.01339
E22=0.01144
E23=0.00975
E24=0.00831
E25=0.00709
E26=0.00604
E27=0.00515
E28=0.00439
E29=0.00375
E30=0.00319
E31=0.00272

```

```

B32=0.00232
B33=0.00198
B34=0.00169
B35=0.00144
B36=0.00123
B37=0.00105
B38=0.00089
B39=0.00076
B40=0.00065
Z1=0.0
Z2=0.C
Z3=0.C
Z4=0.0
Z5=0.C
Z6=0.0
Z7=0.C
Z8=0.0
Z9=0.0
Z10=0.0
Z11=0.C
Z12=0.0
Z13=0.C
Z14=0.0
Z15=0.C
Z16=0.0
Z17=0.C
Z18=0.0
Z19=0.0
E3=0.0
E4=0.C
E5=0.0
E6=0.0
E7=0.0
E9=0.0
E10=0.0
E11=0.C
E12=0.C
E13=0.C
E14=0.C
E15=0.C
E16=0.C
E17=0.C
E18=0.0
E19=0.C
E20=0.0
E21=0.C
E22=0.0
DYNAMIC
E1=1.0
TX=IMPULS(0.0,SAMTIM)
EZ=TX*E1
X1=DELAY(100,SAMTIM,P4)
X2=DELAY(100,SAMTIM,X1)
X3=DELAY(100,SAMTIM,X2)
X4=DELAY(100,SAMTIM,X3)
P1=DELAY(100,SAMTIM,P2)
P4=EZ+A1*X1+A2*X2+A3*X3+A4*X4
PROCEDURE E2,U1=POX(P4)
E2=P4-Y20
U1=-B1*Z1-B2*Z2-B3*Z3-B4*Z4-B5*Z5-B6*Z6-B7*Z7-B8*Z8-B9*Z1 ...
-B10*Z10-B11*Z11-B12*Z12-B13*Z13-B14*Z14-B16*Z16-B17*Z17 ...
-B18*Z18-B19*Z19+B21*E3+B22*E4+B23*E5+B24*E6+B25*E7+B26*E8 ...
+B27*E9+E28*E10+B29*E11+B30*E12+B31*E13+B32*E14+B33*E15 ...

```

```
+B34*E16+B35*E17+B36*E18+B37*E19+B38*E20+B39*E21+B40*E22+B20*E2
Z19=Z18
Z18=Z17
Z17=Z16
Z16=Z15
Z15=Z14
Z14=Z13
Z13=Z12
Z12=Z11
Z11=Z10
Z10=Z9
Z9=Z8
Z8=Z7
Z7=Z6
Z6=Z5
Z5=Z4
Z4=Z3
Z3=Z2
Z2=Z1
Z1=U1
E22=E21
E21=E20
E20=E19
E19=E18
E18=E17
E17=E16
E16=E15
E15=E14
E14=E13
E13=E12
E12=E11
E11=E10
E10=E9
E9=E8
E8=E7
E7=E6
E6=E5
E5=E4
E4=E3
E3=E2
Y20=DELAY(20,20.0,U1)
ENDPRC
PRTPLT E2,P4,E1

TIMER FINTIM=100.,OUTDEL=1.0,DELT=1.0
LABEL LF. BAILEY FOR
ENC
STOP
ENCJOB
```

```

C      MAIN PROGRAM - FILE DIFTST.FOR
C
C      WRITTEN TO SOLVE DIFFERENCE EQUATIONS AND SIMULATE
C      CONTROL SYSTEM FOR ER. D. J. DOWNING BY D.B.NEEDHAM,
C      SEPTEMBER, 1978.
C
C      LANGUAGE - FORTRAN IV
C
C      HOST PROCESSOR - DECSYSTEM-10
C
C      OTHER ROUTINES NEEDED :
C
C          ARIMA - SOLVES ARIMA MODEL
C          FCST - FORCASTS AHEAD FOR POINTS FROM
C                PREVIOUS ARIMA MODEL
C          RANDD - GENERATES N RANDOM NUMBERS
C                WITH NORMAL(0,1) DISTRIBUTION
C          RANDOM- INITIALIZES RANDOM NUMBER
C                SEQUENCE
C
C      TO EXECUTE :
C          EX DIFTST,ARIMA,FCST,RANDD,RANDOM
C
C          REAL*4 NT,NHAT,NTSQ,NTMSE
C          DCUBIE PRECISICN FNAME
C          COMMON NT(1000),PHI(20),THETA(20),NHAT(1000),RAND(1020)
C          DIMENSION WA(1020),START(100)
C          DIMENSION X(1000),OMG(10),GAM(10),E(1000)
C          DATA START/100*0.0/
C          DATA NC/'N'/
C
C      VALUE OF ROOT INITIALIZES RANDOM NUMBER GENERATOR.
C      VALUE MUST BE IN OCTAL -I.E. NO DIGITS GREATER THAN 7.
C
C          DATA ROOT/"35412362773/
C
C      GET ALL NECESSARY PARAMETERS FROM USER.
C
C          TYPE 150
150      FCFORMAT(' BACKSHIFT VALUE ?')
          ACCEPT *,IB
          TYPE 155
155      FORMAT(' NUMBER OF PHI VALUES ?')
          ACCEPT *,NPHI
          IF(NPHI.EQ.0)GO TO 164
          TYPE 160
160      FORMAT(' INPUT THE PHI VALUES, SEPARATED BY COMMAS ')
          ACCEPT *,(PHI(I),I=1,NPHI)
164      TYPE 165
165      FORMAT(' NUMBER OF THETA VALUES ?')
          ACCEPT *,NTHETA
          IF(NTHETA.EQ.0)GO TO 174
          TYPE 170
170      FORMAT(' INPUT THE THETA VALUES, SEPARATED BY COMMAS ')
          ACCEPT *,(THETA(I),I=1,NTHETA)
174      TYPE 175
175      FORMAT(' INPUT NUMBER OF POINTS<= 1000 TO SIMULATE ')
          ACCEPT *,NPTS
          TYPE 180
180      FORMAT(' INPUT MEAN AND VARIANCE, SEPARATED BY COMMAS')
          ACCEPT *,AMEAN,WNV
C
C      GENEPAE NPIS+NPHI RANDOM NORMAL NUMBERS.

```

```

C          CALL RANDD (FOOT,NPTS+NPHI,RAND)
C
C COPY RANDOM NUMBERS INTO WORKING AREA AND
C GENERATE ARIMA SERIES.
C
C          DO 3 I=1,NPTS+NPHI
3          WA(I)=RAND(I)
          CALL ARIMA (PHI,THETA,AMEAN,1.0,START,WNV,NPHI,NTHETA,
                    NPTS,NT,WA)
C
C CALL FORECASTING ROUTINE TO FORECAST B POINTS AHEAD.
C
C          CALL FCSI (IB,NPTS,NPHI,NTHETA)
C
C READ OMEGA AND GAMMA VALUES
C
C          TYPE 300
300         FORMAT (' HOW MANY OMEGA VALUES, INCLUDING OMEGA (0) ?')
          ACCEPT *,NOMG
          TYPE 305
305         FORMAT (' INPUT THE OMEGA VALUES, SEPARATED BY COMMAS')
          ZOM=C.0
          NOMG=NCHG-1
          IF (NOMG.EQ.0) GO TO 308
          IF (NOMG.EQ.-1) GO TO 309
          ACCEPT *,ZOM,(OMG(I),I=1,NOMG)
          GO TO 309
308         ACCEPT *,ZOM
309         TYPE 310
310         FORMAT (' HOW MANY GAMMA VALUES ?')
          ACCEPT *,NGAM
          IF (NGAM.EQ.0) GO TO 388
          TYPE 315
315         FORMAT (' INPUT THE GAMMA VALUES, SEPARATED BY COMMAS')
          ACCEPT *,(GAM(I),I=1,NGAM)
C
C LOAD WORKING AREA WITH NEGATIVE OF FORECASTED ARRAY.
C
388         DO 340 I=1,NPTS
340         WA(I)=-NHAT(I)
C
C CALL ARIMA ROUTINE TO GENERATE CONTROL ARRAY.
C
C          CALL ARIMA (OMG,GAM,0.0,ZOM,START,1.0,NOMG,NGAM,NPTS,X,WA)
C
C GENERATE ERROR ARRAY FROM DIFFERENCE OF OBSERVED AND
C FORECASTED VALUES.
C          DO 875 I=1,NPTS
875         E(I)=NT(I)-NHAT(I)
C
C CALCULATE MSE FOR N(T) AND E(T)
C
C          NTSQ=0.0
          ETSQ=0.0
          DO 880 I=1,NPTS
          NTSQ=NTSQ + NT(I)*NT(I)
          ETSQ=ETSQ + E(I)*E(I)
880         CONTINUE
          AP=NPTS
          NTMSE=NTSQ/AP
          EMSE=ETSQ/AP
C

```

```

C PRINT ALL PARAMETERS AND RESULTS
C
      WRITE(36,5) (PHI(I),I=1,NPHI)
5     FORMAT(' PHI VALUES ', 10(1X,F8.4))
      WRITE(36,10) (THETA(I),I=1,NTHETA)
10    FORMAT(' THETA VALUES ', 10(1X,F8.4))
      WRITE(36,12) ZOM
12    FORMAT(' OMEGA(O) ',F8.4)
      WRITE(36,13) (OMG(I),I=1,NOMG)
13    FORMAT(' OMEGA VALUES ',10(1X,F8.4))
      WRITE(36,14) (GAM(I),I=1,NGAM)
14    FORMAT(' GAMMA VALUES ',10(1X,F8.4))
      WRITE(36,15) IB
15    FORMAT(5X,'B ',I2,/)
      WRITE(36,580)
580   FORMAT(6X,'N(T)',8X,'A(T)',7X,'N(T) HAT',6X,'X(T)',
*      8X,'E(T)',6X,'TIME',//)
      DO 800 I=1,NPTS
      WRITE(36,570) NT(I),RAND(I),NHAT(I),X(I),E(I),I
570   FORMAT(5(4X,F8.4),4X,I4)
800   CONTINUE
      WRITE(36,575) NIMSE,EMSE
575   FORMAT(/,' MEAN SQUARE ERRORS :',/,10X,'N(T) :',
*      E15.5,/,10X,'E(T) :',E15.5)
C
C OUPUT NT & ET TO PLOT FILE
C
      TYPE 200
200   FORMAT(' DO YOU WANT A PLOT FILE OF N(T) & E(T) ? (Y,N)')
      ACCEPT 205,IANS
205   FORMAT(A1)
      IF(IANS.EQ.NO) STOP
      TYPE 210
210   FORMAT(' FILE NAME?')
      ACCEPT 215,FNAME
215   FORMAT(A10)
      OPEN(UNIT=40,ACCESS='SEQOUT',FILE=FNAME)
      DO 216 I=1,NPTS
216   WA(I)=I
      WRITE(40,218) (WA(I),I=1,NPTS)
      WRITE(40,218) (WA(I),I=1,NPTS)
218   FORMAT(10(1X,F6.1))
      WRITE(40,225) (NT(I),I=1,NPTS)
      WRITE(40,225) (E(I),I=1,NPTS)
225   FORMAT(5(1X,F13.5))
      CALL EXIT
      END
C SUBROUTINE ARIMA(ARPS,PMAS,PMAC,ZOM,START,WNV,IP,IQ,LW,W,WA)
C
C
C FUNCTION - GENERATE A TIME SERIES FOR A GIVEN ARIMA
C STOCHASTIC MODEL.
C USAGE - CALL ARIMA (ARPS,PMAS,PMAC,ZOM,START,WNV,
C IP,IQ,LW,W,WA)
C PARAMETERS ARPS - INPUT VECTOR OF LENGTH IP CONTAINING THE
C AUTOREGRESSIVE PARAMETERS OF THE MODEL.
C PMAS - INPUT VECTOR OF LENGTH IQ, CONTAINING
C THE MOVING AVERAGE PARAMETERS OF THE MODEL.
C PMAC - INPUT OVERALL MOVING AVERAGE PARAMETER.
C START - INPUT VECTOR OF LENGTH IP CONTAINING STARTING
C VALUES WITH WHICH TO GENERATE THE TIME
C SERIES.
C WNV - INPUT WHITE NOISE VARIANCE.

```

```

C          IP - INPUT NUMBER OF AUTOREGRESSIVE PARAMETERS
C          IN THE MODEL.
C          IQ  - INPUT NUMBER OF MOVING AVERAGE PARAMETERS IN
C          THE MODEL.
C          LW  - INPUT LENGTH OF THE TIME SERIES TO BE
C          GENERATED.
C          W   - OUTPUT VECTOR OF LENGTH LW CONTAINING THE
C          GENERATED TIME SERIES.
C          WA  - SERVES AS A WORKSPACE. LENGTH
C          EQUAL TO LW+MAX(IP,IQ) .
C LANGUAGE   - FORTRAN
C-----
C
C          SUBROUTINE ARIMA (ARPS,PMAS,PMAC,ZOM,START,WNV,IP,IQ,LW,W,WA)
C
C          DIMENSION      ARPS(IP),PMAS(IQ),START(IP),W(LW),WA(1)
C                          GENERATE WHITE NOISE SERIES
C
C          LZ=LW+IQ
C          SWNV=SCR1(WNV)
C          DO 5  I=1,LZ
C             WA(I)=WA(I)*SWNV
C          5  CONTINUE
C          DO 15 I=1,LW
C             IIQ=I+IQ
C             W(I)=PMAC+WA(IIQ)
C             IF (IQ.EQ.0) GO TO 15
C
C          COMPUTE MOVING AVERAGE CONTRIBUTIONS
C
C          DO 10 J=1,IQ
C             W(I)=W(I)-PMAS(J)*WA(IIQ-J)
C          10  CONTINUE
C          15 CONTINUE
C          IF (IP.EQ.0) GO TO 35
C          DO 20 I=1,IP
C             WA(I)=START(I)
C          20 CONTINUE
C
C          COMPUTE AUTOREGRESSIVE CONTRIBUTIONS
C
C          DO 25 I=1,LW
C             IIP=I+IP
C             WA(IIP)=W(I)
C             DO 25 J=1,IP
C                WA(IIP)=WA(IIP)*ZOM+ARPS(J)*WA(IIP-J)
C          25 CONTINUE
C          DO 30 I=1,LW
C             W(I)=WA(I+IP)
C          30 CONTINUE
C          GO TO 38
C          DO 40 I=1,LW
C             W(I)=W(I)*ZOM
C          40 CONTINUE
C          38 RETURN
C          END
C          SUBROUTINE FCST
C
C          USED TO FCFCST AHEAD B POINTS GIVEN PHI AND
C          THETA PARAMETERS AND NUMBER OF POINTS REQUIRED.
C          ALSO REQUIRED IS ARRAY OF ORIGINAL DATA TO FORCAST FROM.
C
C          SUBROUTINE FCST(IB,NPTS,NPHI,NTHETA)
C          REAL*4 NT,NHAT,NTEMP
C          COMMON NT(1000),PHI(20),THETA(20),NHAT(1000),RAND(1020)
C          DIMENSION NTEMP(1000)
C
C          ZERO OUTPUT ARRAY FOR FIRST B POINTS.

```

```

C
      DO 100 I=1,IB
100    NHAT(I)=0.0
C
C   COPY FIPST E-1 POINTS INTO WORKING BUFFER
C
      DO 500 II=1,NPHI-1
500    NTEMP(II)=NT(II)
C
C   OUTER LOOP 505 CONTROLS NUMBER OF HISTORICAL DATA POINTS
C   USED TO FORECAST FROM
C
      DO 505 I=1,NPTS-IB
C
C   ADD NEXT N(T) TO TEMPORARY BUFFER
C
      NTEMP(I)=NT(I)
C
C   LOOP 510 CALCULATES ALL TEMPORARY TERMS NECESSARY TO FORECAST
C   IB POINTS AHEAD
C
      DC 510 J=1,IB.
          IJ=I+J
          IST=IJ-1
          SUM1=0.0
          IF(NPHI.EQ.0)GO TO 522
C
C   LOOP 520 MAKES PHI*N(T) OR PHI*N(T) HAT CALCULATIONS
C   FOR EACH TEMPORARY TERM
C
          DO 520 K=1,NPHI
              IF(IST.LE.0)GO TO 520
              SUM1=SUM1+PHI(K)*NTEMP(IST)
520          IST=IST-1
C
C   IF MORE THAN NTHETA+1 TEMPORARY TERMS HAVE BEEN CALCULATED,
C   THE THETA*RAND TERMS NO LONGER HAVE ANY EFFECT AND ARE NOT
C   CALCULATED
C
          IF(NTHETA.EQ.0)GO TO 550
          IF(J.GT.NTHETA+1)GO TO 550
C
C   LOOP 530 CALCULATES THE SUM OF THE THETA*RAND TERMS
C
          SUM2=0.0
          ITST=IJ-1
          DO 530 L=1,NTHETA
              IF(ITST.GT.I)GO TO 530
              IF(ITST.LE.0)GO TO 530
              SUM2=SUM2+THETA(L)*RAND(ITST)
530          ITST=ITST-1
C
C   COMPUTE N(T) HAT FOR THIS TEMPORARY STEP
C
          NTEMP(IJ)=SUM1-SUM2
          GO TC 510
550          NTEMP(IJ)=SUM1
C
C   ESTIMATE AT POINT TIME + IB HAS BEEN CALCULATED; STORE AND
C
510          CONTINUE
505          NHAT(IJ)=NTEMP(IJ)
          RETURN

```

```

      END
C
C SUBROUTINE RANDD
C
C CALCULATES UP TO 1000 RANDOM NORMAL NUMBERS, NORMALLY DISTRIBUTED
C WITH MEAN 0 AND VARIANCE 1. THE SEQUENCE GENERATED DEPENDS
C ON THE VALUE OF 'ROOT' WHICH SHOULD BE SUPPLIED IN OCTAL.
C VECTOR RAND IS RETURNED CALCULATED THROUGH NPTS
C NUMBER OF PCINTS.
C
      SUBROUTINE RANDD (ROOT,NPTS,RAND)
      DIMENSION RAND(1000)
      CALL RANDIN(ROOT)
      DO 100 I=1,NPTS
100   RAND(I)=RANX(DUMMY)
      RETURN
      END
      FUNCTION RANX(DUMMY)
      R = FLTRN(R)
      IF(R .GT. 0.8638) GO TO 10
      RANX = 2.*(PLTRN(X) + PLTRN(Y) + PLTRN(Z) - 1.5)
      RETURN
10   IF( R.GT. 0.9745) GO TO 20
      RANX = 1.5*(PLTRN(X) + PLTRN(Y) - 1.0)
      RETURN
20   IF(R .GT. 0.997302039) GO TO 100
25   X = 6. *PLTRN(X) - 3.0
      Y = 0.358*PLTRN(X)
      XSQ = X*X
      GX = 17.4931196*EXP(-XSQ*0.5)
      AX = AES(X)
      IF(AX .GT. 1.0) GO TO 30
      IF(Y.GI.(GX-17.44392294+4.73570326*XSQ+2.15787544*AX)) GOT025
      RANX = X
      RETURN
30   AX3 = 2.36785163*(3-AX)**2
      IF(AX .GT. 1.5) GO TO 40
      IF(Y .GT. (GX-AX3-2.15787544*(1.5-AX))) GO TO 25
      RANX = X
      RETURN
40   IF(Y .GT. (GX-AX3)) GO T025
      RANX = X
      RETURN
100  X = SQRT(9-ALOG(PLTRN(X)))
      IF(PLTRN(X) .GT. 3/X) GO TO 100
      IF(PLTRN(X) .GT. 0.5) X = -X
      RANX = X
      RETURN
      END
      TITLE RANDOM
      TO==0
      T1==1
      L==16
      P==17
      ENTRY RANDIN
RANDIN: SETZ TO,
      MOVE TO,20(L)
      MOVEM TO,ARG
      POPJ P,
      ENTRY FLTRN
FLTRN: MOVE TO,ARG
      MUL TO,ARGC

      MOVEM T1,ARG
      LSH T1,11
      LSH T1,-11
      FSC T1,200
      MOVE TO,T1
      POPJ P,
ARGC: EXP DE30517578125
ARG: EXP 343277244615
      END

```

APPENDIX B

KALMAN FILTER

One is motivated to seek the "best" estimate of the level of the manufacturing process. In a manufacturing process the available information at some period, t , is 1) the history of measurements, $\{Y(i): i=0,1,\dots,t\}$, and 2) measurement errors on the measure of interest. In the typical manufacturing process, this is the maximum amount of data that is available. From this data, one must devise a technique to extract as much information as possible about the true level of the process.

One could attempt to estimate the mean level of the process by forming a linear function of the available measurements:

$$\mu(t) = \sum_{i=0}^t \underline{a}_i(t)y(i) . \quad (\text{B.1})$$

By specifying the coefficients $\underline{a}_i(t)$ in (B.1), one has the optimal estimate. One way of choosing the coefficients in (B.1) is to form an expression for the variance of the error of the state estimate and choose the $\underline{a}_i(t)$ to minimize this error variance. This approach would utilize all available information about the process to produce an optimal estimate of the variable of interest. If the additional constraint that the estimate be unbiased is imposed, the minimum variance estimate is equivalent to a least squares estimate.

Note that, to implement the estimation technique in (B.1), one has to calculate the optimal coefficients. One must maintain the entire history of measurements and measurement variances. Thus, to implement the optimal policy, one must perform some formidable calculations and maintain a rather large data file.

Fortunately, there is an alternate way of implementing the policy defined by (B.1). This is by means of the Kalman Filter. The Kalman Filter approach has several advantages over the policy defined by (B.1):

- 1) The iterative equations are somewhat easier to implement.
- 2) The iterative procedure produces an error covariance matrix as a by-product.
- 3) The entire history need not be maintained. Rather, one maintains the most recent state estimate and the associated error covariance matrix which contain all relevant information about the process history.

There are four key elements in the Kalman Filter:

- 1) A system state vector: the state vector at time t , $\underline{X}(t)$ includes as a minimum the mean of the process.
- 2) A system model: a linearized set of equations of the form:

$$\underline{X}(t+1) = \underline{A}(t)\underline{X}(t) + \underline{U}(t) + \underline{C}(t) . \quad (\text{B.2})$$

There is one equation for each state variable. One equation is a mass balance equation which describes how the process evolves in time. $\underline{U}(t)$ is a known "control vector". The vector $\underline{C}(t)$ is a zero mean random vector which is used to account for imperfect knowledge of $\underline{U}(t)$ and/or modeling errors. To account for process measurement errors, the following equation is used:

$$\underline{Y}(t) = \underline{H}(t)\underline{X}(t) + \underline{V}(t) , \quad (\text{B.3})$$

where $\underline{V}(t)$ is a zero mean random vector, and $\underline{H}(t) = [1]$.

- 3) Measurements: process level (e.g., U^{235} content).
- 4) Variances: process and measurement.

The Kalman Filter produces state estimates which minimize a sum of terms, each term being the error variance of a component of the state vector.

In summary, the Kalman Filter is applicable to a linear system of the form of Equations (B.2) and (B.3) with known transition matrix $\underline{A}(t)$. The measurement covariance matrix of $\underline{Y}(t)$, $\underline{R}(t)$, as well as the process covariance matrix for $\underline{X}(t)$, $\underline{Q}(t)$, must be known. The random vectors $\underline{C}(t)$ and $\underline{V}(t)$ in the model have zero cross correlation.

The listing below constitutes the iterative procedure known as the Kalman Filter:

- 1) Choose $\hat{\underline{X}}(0)$, an unbiased estimate of $\underline{X}(0)$, and $\underline{G}(0)$, a positive definite symmetric error covariance matrix. Set $t=1$.
- 2) State Prediction:

$$\tilde{\underline{X}}(t) = \underline{A}(t-1)\hat{\underline{X}}(t-1) + \underline{U}(t-1) . \quad (\text{B.4})$$

- 3) Calculate error covariance matrix for state estimate in last step:

$$\underline{P}(t) = \underline{A}(t-1)\underline{G}(t-1)\underline{A}(t-1)^T + \underline{Q}(t-1) . \quad (\text{B.5})$$

- 4) Calculate gain:

$$\underline{K}(t) = \underline{P}(t)\underline{H}(t)^T [\underline{H}(t)\underline{P}(t)\underline{H}(t)^T + \underline{R}(t)]^{-1} . \quad (\text{B.6})$$

- 5) Update state estimate:

$$\hat{\underline{X}}(t) = \tilde{\underline{X}}(t) + \underline{K}(t)[\underline{Y}(t) - \underline{H}(t)\tilde{\underline{X}}(t)] . \quad (\text{B.7})$$

- 6) Calculate error covariance matrix for the state estimate in the last step:

$$\underline{G}(t) = [\underline{I} - \underline{K}(t)\underline{H}(t)]\underline{P}(t) . \quad (\text{B.8})$$

Figure B.1 shows the flow chart for implementing the Kalman Filter.

Using $E(\)$ to denote the expectation operator and $\underline{e}(t)$ to denote the error, $\underline{x}(t) - \hat{\underline{x}}(t)$, the choice of $\underline{K}(t)$ is such that $E[\underline{e}(t)\underline{e}(t)^T]$, the trace of $\underline{G}(t)$, is minimized. Matrices $\underline{P}(t)$ and $\underline{G}(t)$ are error covariance matrices. $\underline{P}(t)$ is the error covariance matrix of $\underline{e}(t)$ given $\{Y(j): j=1,2,\dots,t-1\}$:

$$\underline{P}(t) = E\{\underline{e}(t)\underline{e}(t)^T / Y(1), \dots, Y(t-1)\} . \quad (\text{B.9})$$

The matrix $\underline{G}(t)$ is the error covariance matrix given $\{Y(j): j=1,2,\dots,t\}$:

$$\underline{G}(t) = E[\underline{e}(t)\underline{e}(t)^T / Y(1), \dots, Y(t)] . \quad (\text{B.10})$$

Thus, $\underline{P}(t)$ is the error-covariance matrix before receipt of the observation at time t , while $\underline{G}(t)$ is the error-covariance matrix after receipt of the observation at time t .

The approach taken in deriving the Kalman Filter is that of minimizing the trace of $\underline{G}(t)$. The same results, however, can be obtained from a number of approaches including:

- 1) Minimizing Bayesian Decision Theory
- 2) Minimizing the length of the error vector squared
- 3) Maximum Likelihood estimation.

The latter two methods require the assumption of normality for the measurement and process errors. The approaches which minimize the trace

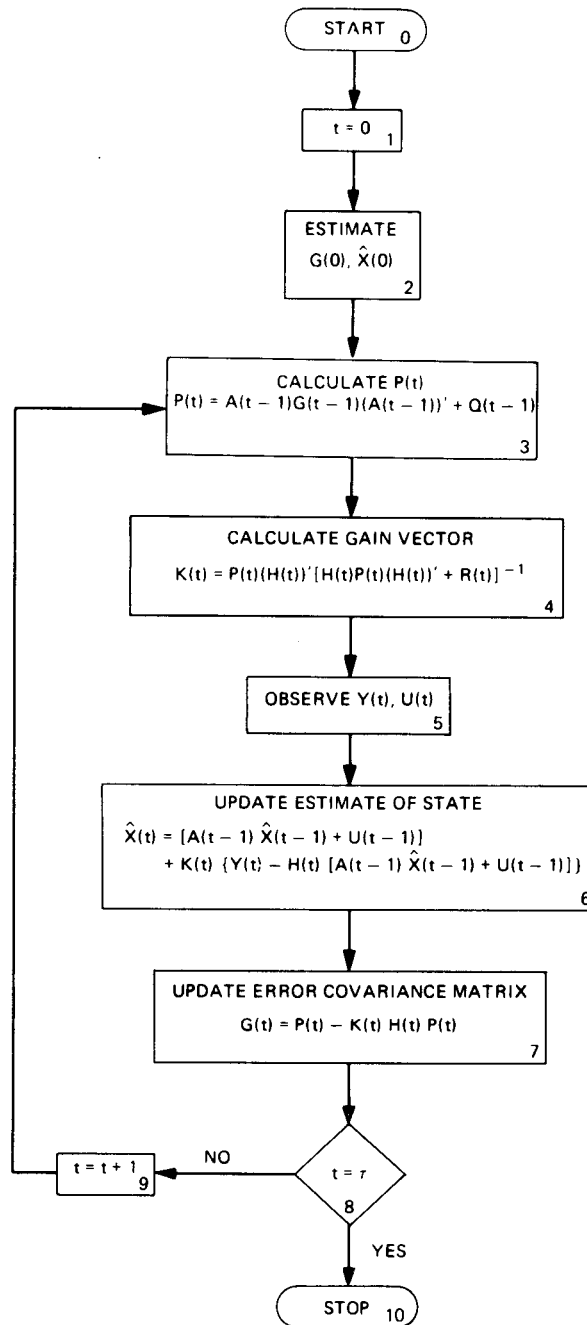


Fig. B.1. Flow Chart of the Kalman Filter.

of $\underline{G}(t)$ or which minimize the length of the error vector (which is, in fact, the same as the trace of $\underline{G}(t)$) do not require the assumption of normality. It should be noted that when the assumption of normality holds, the Kalman Filter 1) minimizes the trace of $\underline{G}(t)$, 2) is the maximum likelihood estimate, and 3) is the optimum Bayesian estimate. It has also been shown that under the assumption of normality, no other estimate (neither linear nor nonlinear) is superior to the Kalman Filter. If the assumption of normality does not hold, the optimal linear estimate is the Kalman Filter, but there may be a nonlinear estimate which is superior.

Kalman Filter Applied to Estimating Mean Process Level in Fuel Rod Fabrication

As an example of the use of the Kalman Filter, consider the problem of improving the assay measurements by filtering. The system model is:

$$\mu(t+1) = \mu(t) \quad (\text{B.11})$$

where $\mu(t)$ = system state variable = mean U^{235} content at start of period t . Equation (B.11) is a mass balance equation which must hold in the absence of process changes in level. It simply states that the process level does not change with time. The measurement equation is:

$$Y(t) = \mu(t) + V(t) \quad (\text{B.12})$$

where $V(t)$ = measurement error for U^{235} content.

In this case, the Kalman Filter reduces to:

- 1) Initialization: $\hat{\mu}(0) = Y(0)$. $G(0) = R(0)$. That is, we are setting the initial state estimate equal to the initial

measurement of the U^{235} content. The error covariance matrix is the measurement error.

2) Gain:

$$K(t) = G(t-1)/[G(t-1) + R(t)] \quad (B.13)$$

where $R(t)$ equals process error plus measurement error at time t .

3) State Update:

$$\mu(t) = \mu(t-1) + K(t)[Y(t) - \mu(t-1)] \quad (B.14)$$

4) Error Covariance Matrix for $\mu(t)$:

$$G(t) = \frac{R(t)G(t-1)}{G(t-1) + R(t)} \quad (B.15)$$

Equations (B.13—B.15) constitute the Kalman Filter for producing the estimate of U^{235} content. The filter acts so as to produce minimum variance estimates; i.e., the error variance, $G(t)$, is minimized.

ORNL/CSD/TM-87
Dist. Category UC-77

INTERNAL DISTRIBUTION

- | | | | |
|--------|--|--------|--------------------------------------|
| 1. | E. J. Allen | 17. | D. H. Pike |
| 2. | P. Angelini | 18. | J. E. Rushton |
| 3-5. | Milton Bailey | 19. | R. R. Suchomel |
| 6. | B. J. Bolfig | 20. | G. W. Westley |
| 7. | A. J. Caputo | 21. | D. F. Williams |
| 8. | H. P. Carter/A. A. Brooks/
CSD X-10 Library | 22-23. | Central Research Library |
| 9. | D. A. Costanzo | 24. | Document Reference
Section - Y-12 |
| 10-12. | D. J. Downing | 25-27. | Laboratory Records |
| 13. | D. R. Johnson | 28. | Laboratory Records -
Record Copy |
| 14. | F. Kitts | 29. | ORNL Patent Office |
| 15. | W. J. Lackey | | |
| 16. | S. R. McNeany | | |

EXTERNAL DISTRIBUTION

30. J. N. Rogers, Division 8324, Sandia Laboratories, Livermore California 94550.
31. Chief, Mathematics and Geoscience Branch, Department of Energy Mathematical and Computer Sciences Program, Molecular Sciences and Energy Research, Division of Physical Research, Washington, D. C. 20545.
32. Office of Assistant Manager for Energy Research and Development, Department of Energy, Oak Ridge Operations, Oak Ridge, Tennessee 37830.
- 33-208. Given Distribution as shown in TID-4500 under UC-77, Gas Cooled Reactor Technology